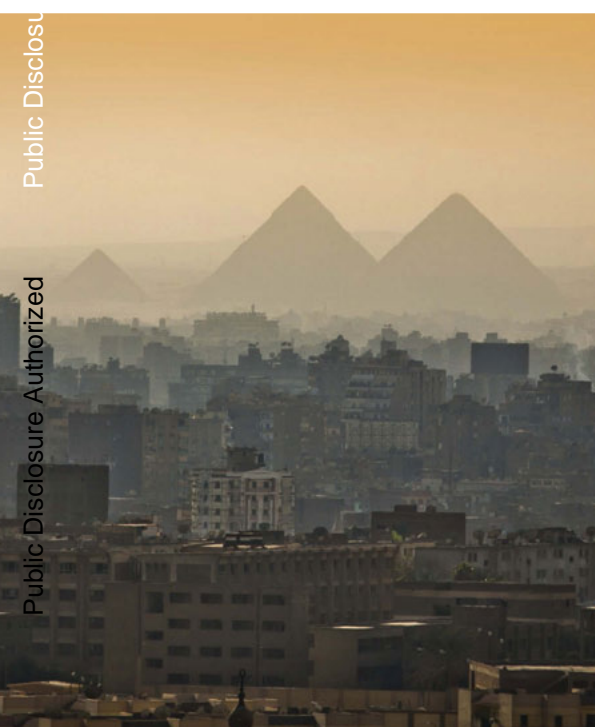


MOTOR VEHICLE DENSITY AND AIR POLLUTION IN GREATER CAIRO

Fuel Subsidy Removal & Metro Line Extension and their Effect on Congestion and Pollution



MOTOR VEHICLE DENSITY AND AIR POLLUTION IN GREATER CAIRO

FUEL SUBSIDY REMOVAL AND METRO LINE EXTENSION & THEIR EFFECT
ON CONGESTION AND POLLUTION?

Martin Heger,^a David Wheeler,^a Gregor Zens,^{a,b} and Craig Meisner^a

^aEnvironment and Natural Resources Global Practice, The World Bank Group

^bDepartment of Economics, Vienna University of Economics and Business

© 2019, The World Bank
818 H Street N.W,
Washington DC 20433
Telephone: (202)473 1000
Internet: www.worldbank.org
Some rights reserved

This work is a product of the staff of the World Bank with external contributions. Note that the World Bank does not necessarily own each component of the content included in the work. The World Bank therefore does not warrant that the use of the content contained in the work will not infringe on the rights of third parties. The risk of claims resulting from such infringement rests solely with you.

This report is a product of The World Bank. It reflects the findings of the World Bank study team, and does not necessarily represent the views of the Ministry of Environment of Egypt and its Egyptian Environmental Affairs Agency (EEAA).

The findings, interpretations, and conclusions expressed in this work do not necessarily reflect the views of the World Bank, its Board of Executive Directors, or the governments they represent. The World Bank does not guarantee the accuracy of the data included in this work. The boundaries, colors, denominations, and other information shown on any map in this work do not imply any judgment on the part of the World Bank concerning the legal status of any territory or the endorsement or acceptance of such boundaries. Nothing herein shall constitute or be considered to be a limitation upon or waiver of the privileges and immunities of the World Bank, all of which are specifically reserved.

Rights and Permissions

This work is available under the Creative Commons Attribution 3.0 Unported license (CC BY 3.0) <http://creativecommons.org/licenses/by/3.0>. Under the Creative Commons Attribution license, you are free to copy, distribute, trans-mit, and adapt this work, including for commercial purposes, under the following conditions:

Attribution—Please cite the work as follows: Heger, Martin; Wheeler, David; Zens, Gregor; and Meisner, Craig. 2019. *Motor Vehicle Density and Air Pollution in Greater Cairo: fuel subsidy removal and metro line extension & their effect congestion and pollution?* The World Bank.

All queries on rights and licenses should be addressed to the Office of the Publisher, The World Bank, 1818 H Street NW, Washington, DC 20433, USA; fax: 202-522-2625; e-mail: pubrights@worldbank.org.

TABLE OF CONTENTS

Acknowledgments	v
Summary	vi
CHAPTER ONE: Air Pollution and Traffic in Greater Cairo	1
CHAPTER TWO: Recent Research on Environmental Policies	4
2.1 Public Transport and Environmental Measures	4
2.2 Responses to Fuel Price Shocks	5
CHAPTER THREE: Empirical Approach	6
CHAPTER FOUR: Data	8
4.1 Vehicle Counts	8
4.2 Ground Monitoring Air Quality Measurement	10
4.3 Information about the Policy Shocks	10
4.4 Control Variables	12
CHAPTER FIVE: Results	14
5.1 The Impact of Recent Policy Measures on Traffic Density in Cairo	14
CHAPTER SIX: The Impact of (Environmental) Policy on Car Traffic, Air Pollution, and Health	22
6.1 Illustrative Events in Cairo	26
6.2 Value of Health Benefits Resulting from PM ₁₀ Reduction	32
CHAPTER SEVEN: Summary and Conclusions	34
References	35
Technical Appendix	38
A1. Vehicle Counts	38
A2. Satellites	38

FIGURES

Figure 1: PM₁₀ Concentrations (5 Months Moving Average) in Greater Cairo, 2010–2016	1
Figure 2: PM_{2.5} Sources in Greater Cairo	2
Figure 3: Schematic of Machine Learning Algorithm Detecting Cars in the Streets of Cairo on a Stretch of a Highway and at a Neighborhood Scale	9
Figure 4: Car Density in the Streets of Cairo during an Average Weekday	10
Figure 5: Location of Air Quality Monitoring Stations	11
Figure 6: Cairo Metro Lines	12
Figure 7: Estimated Coefficients and 95% CIs for All Time Windows	18

Figure 8a: Spatial Distribution of Car Counts Prior to the Metro 3 Phase One Opening 27

Figure 8b: Spatial Distribution of Car Count Changes after the Phase One Opening 28

Figure 9a: Spatial Distribution of Car Counts Prior to the November 3
Fuel Price Increase 30

Figure 9b: Spatial Distribution of Car Count Changes after the November 3 Increase 31

Figure A1: Grid Overlay in Greater Cairo 39

TABLES

Table 1: Fixed-Effects Estimates (Cluster Standard Errors): Determinants
of Cairo Vehicle Counts per Cell 17

Table 2: Cell Vehicle Counts and PM₁₀ Concentrations 21

Table 3: Cairo Region: Projected Event Impacts on Traffic Volume. 23

Table 4: Cairo Monitoring Stations: Potential Impact Measure for PM₁₀ Attributable
to the Maximum Sample Car Count 23

Table 5: Estimated Impacts of Policy Measures on Cairo PM₁₀ 24

Table 6: Metro Line 3 Phase 1 Opening, February 21, 2012 26

Table 7: Fuel Price Increase, November 3, 2016: Ex-Ante and Ex-Post Car Densities 29

Table A1: Image Counts per Satellite 38

Table A2: Accuracy Assessment 40

ACKNOWLEDGMENTS



This report is the product of a broad and extensive collaboration between the World Bank and the Ministry of Environment/Egyptian Environmental Affairs Agency (EEAA). The numerous and rich discussions and exchange of information has been critical for the preparation of this report.

The report drafting team would like to first and foremost acknowledge the invaluable contributions of Moustafa Mourad from the Egyptian Environmental Affairs Agency (EEAA). In addition, very useful comments were received from Heba Shrawy, Hazem El Zanan, and Abir Abuzeid (all at EEAA). The team is most grateful for the continued support of H.E. Dr. Yasmine Fouad, Minister of Environment, and Dr. Khaled Fahmy, the former Minister of Environment.

The team would also like to thank Ben Stewart and the team at Orbital Insight for their invaluable contributions to the Earth Observation and Machine-Learning modelling. Many thanks also to Mr. Benoît Blarel, Practice Manager, Environment and Natural Resources Global Practice, and Ms. Lia Sieghart, Practice Manager, Environment and Natural Resources Global Practice for their guidance. Lastly, the team would like to acknowledge the financial support of this study through the Korean Green Growth Trust Fund (KGGTF) and the Pollution Management and Environmental Health (PMEH) Trust Fund.

SUMMARY



This report answers two questions: What is the statistical relationship between vehicle density in the streets of Greater Cairo and ambient air pollution in the city? And what are the effects of—one, the opening in recent years of another metro line and an extension to it, and two, the recent increases in fuel prices—on vehicle density and ambient air pollution?

A novel dataset created for this report identified vehicles running in the streets of Cairo using trained Machine Learning algorithms based on high-resolution satellite imagery. Nearly every vehicle running in the streets of Cairo was detected and counted on nearly 1,000 days during the period 2010 to 2018. The resulting vehicle data was then used in relation to observations from ground monitors monitoring PM_{10} (particles the size of 10 μm or less in aerodynamic diameter). A statistical model was developed, relating the counted cars to the monitored concentrations of air pollution. The relationship between car density and ambient air pollution was found to be linear, and it was found that reducing the number of cars by 1% led to a corresponding PM_{10} reduction of 0.27%.

Impact evaluation methods were then applied to estimate the effect that policy events (notably the opening of another metro line and the slashing of fuel subsidies) had on air pollution in Egypt. Using fixed-effects panel regression methods, it was found that the fuel subsidy removal programs helped to reduce PM_{10} concentrations by nearly 4%. It was also found that the opening of Cairo's Metro Line 3 resulted in the reduction of air pollution by about 3%. Using established concentration-response relationships from epidemiology literature, it was estimated that these two enacted policies must have helped in the avoidance of a significant incidence of mortality and morbidity.

CHAPTER ONE

AIR POLLUTION AND TRAFFIC IN GREATER CAIRO

Air pollution in the Greater Cairo area is a serious environmental issue in Egypt. Although particulate matter (PM) air pollution has improved significantly in Cairo over the last decade (see Figure 1), air pollution levels remain high throughout the year, and levels of PM exceed World Health Organization (WHO) standards as well as Egypt's legal limits.

FIGURE 1: PM₁₀ CONCENTRATIONS (5 MONTHS MOVING AVERAGE) IN GREATER CAIRO, 2010–2016

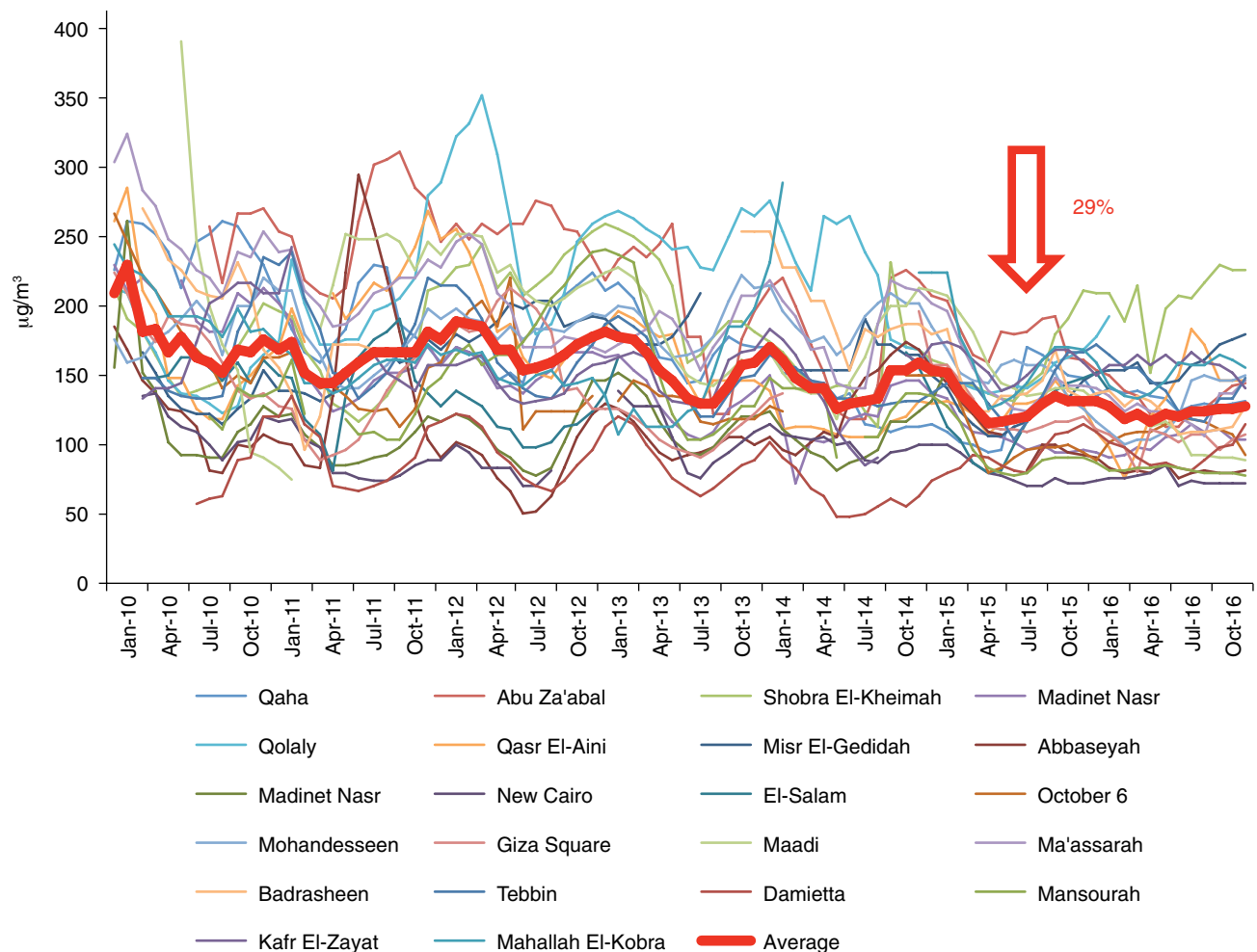
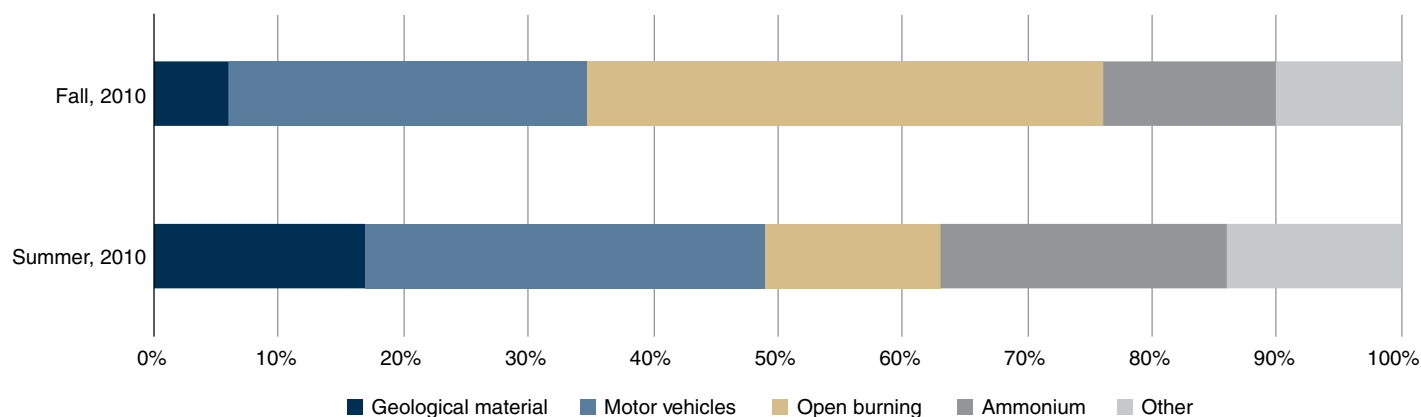


FIGURE 2: PM_{2.5} SOURCES IN GREATER CAIRO



Source: World Bank, 2013.

According to the Ministry of State for Environmental Affairs, the transport sector accounts for about 26% of the PM₁₀ load in Greater Cairo, as well as 90% of carbon monoxide (CO) and 50% of nitrogen oxides (NO_x). The contribution of motor vehicles to PM_{2.5} counts (or counts of fine particles the size of 2.5 µm or less, which are small enough to be an even greater risk to health) are major as well, as seen in Figure 2. The problem is aggravated by poor fuel quality, the average age of cars (two-thirds were older than 15 years in 2010), and the frequent absence of pollution abatement technology.

In principle, environmental problems due to traffic can be addressed via three channels: economic incentives, through for example imposing taxes or lifting subsidies; restrictions on car use; or investment in public transit. In practice, environmental policy in Egypt includes all three of these options. For instance, publicly-mandated fuel price increases (due to the government's lifting of fuel subsidies) have taken place in 2016, 2017, and 2018. Egypt has also recently put into place regulations on the forced retirement of old vehicles via applying age restrictions on transport and passenger cars.¹ But the most significant measure regarding public transit in Cairo has been the opening of a third metro line. For a review of environmental policies in Egypt in the last years, refer to Abou-Ali and Thomas (2011).

This study seeks to inform the wider environmental and transport policy dialogue with an impact analysis for recent economic measures and public transit initiatives. We focus particularly on two publicly-mandated fuel price increases and the two-phased opening of Cairo's Metro Line 3. Our main contributions are threefold: First, we employ high-resolution satellite imagery to produce a spatial panel database of daily vehicle counts in Greater Cairo using trained machine-learning algorithms. Second, we look not only at short-term effects but assess environmental policy effects in the medium to long term. And third, this is one of the first studies anywhere in the world to use panel regression quasi-experimental methods to evaluate the effect of major public transportation policies on traffic and air pollution in the Arab world, and the first to do so in Egypt.

¹These measures were adopted on October 19, 2017, by the Egyptian Cabinet, as part of an amendment to Traffic Law No. 66 of 1973. See <http://english.ahram.org.eg/NewsContent/1/64/279011/Egypt/Politics-/Egypts-cabinet-drafts-first-major-reforms-to-traffic.aspx>

Our analysis is carried out in two econometric exercises: First, we estimate the extent to which recent policy measures have reduced car use in the Greater Cairo area and examine the temporal adjustment pattern of traffic. After that, we estimate the elasticity of cars and PM_{10} pollution to evaluate policy effectiveness in terms of air pollution reduction.

The remainder of the study is organized as follows: Chapter 2 reviews recent international research on public transit and fuel price impacts on car use and air pollution. Chapter 3 describes our empirical approach, and Chapter 4 introduces the data. In Chapter 5, we present estimates of the effects of various policies on car use in the Greater Cairo region and the impact of car use on PM_{10} pollution there. Chapter 6 provides a framework through which to analyze the overall impact of the policies in a counterfactual study. We summarize and conclude the paper in Chapter 7.

CHAPTER TWO

RECENT RESEARCH ON ENVIRONMENTAL POLICIES

2.1 PUBLIC TRANSPORT AND ENVIRONMENTAL MEASURES

Public transit has often been proposed as a measure to counter air pollution and traffic congestion. The basic idea can be traced back to Crowther et al. (1963) in its literature. The underlying rationale is intuitive: More options for public transit will lead more people to use this mode of transport and decrease the share of private options (such as cars or motorbikes). This will in turn decrease average traffic congestion and reduce emissions of air pollutants.

The empirical literature confirms that public transit has significantly affected the numerous variables of interest to researchers and policy makers. Yang et al. (2018) estimate that subway expansions in Beijing reduced traffic delay times by 15% for a prolonged period. One widely-used modeling approach employs strikes of public transport employees to estimate the impact of public transport systems. Using this approach, Anderson (2014) finds that a strike day in Los Angeles may increase traffic delay times by an astonishing 47%. In a study for several U.S. cities, Pang (2018) also finds significant effects on traffic flow in the areas surrounding metro stations. Similarly, Adler and van Ommeren (2016) find increases in traffic congestion on strike days in Rotterdam.

Other studies focus on the air pollution/public transport nexus. Basagaña et al. (2018) find significantly elevated pollution levels on days with public transportation strikes in Barcelona. Chen and Whalley (2012) find significant reduction effects on air pollution after the metro opening in Taipei. Using not only within-city variation but a global dataset of subway openings in combination with satellite-derived pollution data, Gendron-Carrier et al. (2018) find strong and significant effects of metro openings on air pollution in all parts of the world. Overall, they find a reduction of approximately 4% in pollutant measurements in the first months after metro openings. Similar results are found in national studies for Germany (Lalive et al., 2017), China (Zheng et al., 2017), India (Goel and Gupta, 2014) and Canada (Rivers and Plumptre, 2016; Rivers et al., 2017).

Similar studies are relatively rare for countries in the Middle East and North Africa region. Since the region struggles with numerous environmental pollution issues, this knowledge gap has potentially serious consequences for public welfare. In Egypt, for example, air pollution is considered one of the five greatest risk factors for disease and premature death (Wang et al., 2012). An exception to the problem is provided by Tabatabaiee and Rahman (2011), who

explore the effect of urban rail transit on energy consumption and air pollution in Ahvaz, a city of 1.3 million in Iran. Abou-Ali and Thomas (2011) as well as Thomas (2016) review environmental policies in Greater Cairo and provide policy recommendations. They analyze demand for various modes of transport at household levels and conduct a rough analysis to assess the effect of various policies on pollution in Cairo. Abou-Ali and Thomas (2011) find that PM_{10} levels have been reduced by around 3% following the implementation of a set of various policies.

2.2 RESPONSES TO FUEL PRICE SHOCKS

Changes in fuel prices can have a variety of effects on human behavior. These behavioral adjustments are multidimensional (short-term/long-term, local/national, and so on). For instance, the short-term effects of fuel price increases include trip-chaining (combining otherwise separately driven routes) or reorganizing regular trips (for example, a single long shopping trip instead of three short ones). Moreover, preferences with respect to the choice of destination might change, and closer destinations might gain more weight in the decision process (Pendyala, 2010).

In the medium term, people realize that the cost of driving relative to other modes of transport (for instance public transit) increases, which can result in a change in the composition of the vehicle fleet (cars become less frequent and/or more fuel efficient). Long-term effects include the expansion of railway systems, *inter alia*. According to CBO (2008), all of the mentioned factors may have observable impacts on driving behavior and urban traffic patterns.

So far, the only available study on traffic in the Greater Cairo metropolitan area is the Cairo traffic congestion study (World Bank, 2010). This study, however, relies on data that has been collected through a traffic count survey, that is, by manually counting cars at 15 locations in Cairo for three days in the morning and in the afternoon.

On the other hand, most empirical academic studies rely on indirect measurements of individual transport responses to fuel price changes. Common approaches include using car ownership or car travel data compiled from surveys to estimate car ownership elasticities (Dargay and Vythoulkas (1999), Fridstrøm (1998)). This literature shows that car ownership declines with increasing car running costs, including fuel costs. Others estimate the fuel price elasticity of demand using fuel consumption data. Graham and Glaister (2002) estimate long-run price elasticities of car running costs between -0.6 and -1.2 for various European countries. Studies that directly employ vehicle-level data are comparatively rare. One example is Gillingham (2014), who analyzes a vehicle-level dataset in California, constructing a database of over 2 million vehicles from official registers and using the number of vehicle miles traveled between the date-of-purchase and a mandatory smog check as a dependent variable. The medium-term estimate of the elasticity of vehicle miles traveled and fuel prices is -0.22 for new vehicles. For a thorough review of the empirical literature on the relationship between fuel consumption and traffic, refer to Goodwin et al. (2004).

CHAPTER THREE

EMPIRICAL APPROACH

Our investigation focuses on two econometric exercises. First, we assess the effects of the Cairo metro's expansion and of the fuel price hikes (as a reaction to the cutting of fuel price subsidies) on Cairo traffic using fixed-effects panel regressions. Our event-based study design evaluates the sharp discontinuity imposed on the outcome variable (car density) on account of the policy interventions evaluated. In addition, we use a similarly specified model using temporal subsets of the data to examine the temporal adjustment process of Cairo traffic following policy shocks.

Our second econometric exercise uses a sample of PM_{10} measures recorded from eight Cairo monitoring stations during 2016 and 2017. Our fixed-effects panel model relates measured PM_{10} concentrations to car counts in the areas surrounding the stations.

The statistical approach of our first study is a classical discontinuity-based panel regression of the form

$$vehicles_{i,t} = \alpha + \beta x_{i,t} + \delta_1 z_{1,i,t} + \dots + \delta_q z_{q,i,t} + \gamma_i + \epsilon_{i,t}$$

where i denotes a raster tile and t denotes the day of the observation. $vehicles_{i,t}$ is the number of cars in a raster tile i on a given day t . x contains a variety of standard control variables discussed below. γ_i are tile fixed effects. z_q is a set of dummy variables that take the value of 1 for a given time period after the date a specific event q occurs. For the policy interventions, the value of the variable is 0 from the sample start to the day before the intervention and 1 thereafter. Therefore, the coefficients of main interest are δ_q , which are the estimates of the effects that the events in set q had on the outcome variable of interest (car density). Using this setup, we are able to check for a structural break (that is, a level shift) in the time series after the events examined in our study occurred. For comparable approaches in similar settings, see Chen and Whalley (2012) or Gendron-Carrier et al. (2018).

In an additional specification, we explore the adjustment dynamics of traffic adaption in Cairo following the opening of the new metro stations. A two-step estimation procedure is employed. At first, we residualized the car count data and the respective policy event variable using the control variable set discussed below, as well as the policy variables not under examination. Regressing the residualized car counts on the residualized policy variable will yield the same estimate as in the full model specification. This is widely known as the Frisch Waugh Lovell theorem (for example, Lovell 2008). We are interested in the adjustment dynamics of

traffic in Cairo, however, and not in reproducing estimates of the model discussed above. Therefore, we restricted our analysis to temporal subsets of the data set. The subsets were chosen based on various short-term time windows, for instance ± 3 months around the metro openings. More formally, we estimate

$$\begin{aligned} Cars_{it} &= \alpha + \beta x_{it}^* + \tau_{it} \\ Metro_t &= \gamma + \delta x_t^* + \omega_t \\ \tau_{it} &= \zeta \omega_t + \epsilon_{it} \end{aligned}$$

where x_{it}^* and x_t^* are the sets of control variables excluding the policy dummy under analysis. $Metro_t$ is a dummy variable that takes the value of 0 before the metro opening and the value of 1 from the day the metro opened onward. Note that this model is estimated separately for metro phase 1 and phase 2. The first two equations are estimated using the full dataset, and the third equation is estimated using a temporal subset of the data. The coefficient of interest is ζ , which gives us the marginal effect of the respective metro opening on car counts in Cairo.

Our second econometric exercise uses a sample of PM_{10} measures recorded from eight Cairo stations during 2016 and 2017. Our model relates measured PM_{10} concentrations to mean car counts in the grid cells surrounding the monitoring station locations. In formal terms, we estimate

$$PM_{10i,t} = \alpha + \beta vehicles_{i,t} + \zeta x_{i,t} + \gamma_i + \epsilon_{i,t}$$

where $PM_{10i,t}$ denotes the PM_{10} measurement of station i on day t , and $vehicles_{i,t}$ is the mean car count for the tiles surrounding station i on day t . Again, $x_{i,t}$ is a set of control variables as discussed below. γ_i are station fixed effects and $\epsilon_{i,t}$ is a standard i.i.d. error term. The vehicle count variable enters the model in different specifications. We experiment with logarithmic and nonlinear models of the relationship between car counts and PM_{10} concentrations, using both continuous nonlinear forms and linear and nonlinear spline models. We find that none of the alternative models performs as well as the pure linear model.

CHAPTER FOUR

DATA

The three most important variables in our analysis are: (i) car density, which we derive from high-resolution satellite images using trained machine learning algorithms; (ii) particulate matter ambient air pollution concentrations, which we have sourced from the Egyptian Environmental Protection Agency; and, (iii) information on the policy shocks we evaluated, which we extracted from public documents.

4.1 VEHICLE COUNTS

The authors partnered with a remote sensing company,² which applied a trained Machine Learning algorithm to satellite imagery of Cairo, counting every car in the metropolis's streets for each available day³ from January 2010 to April 2018 using a grid. For an illustration of the algorithm identifying vehicles (car detection is depicted with a green spot, and bus/truck detection is depicted with a purple dot), see Figure 3. An example for mapping car density during an average weekday is illustrated in Figure 4.

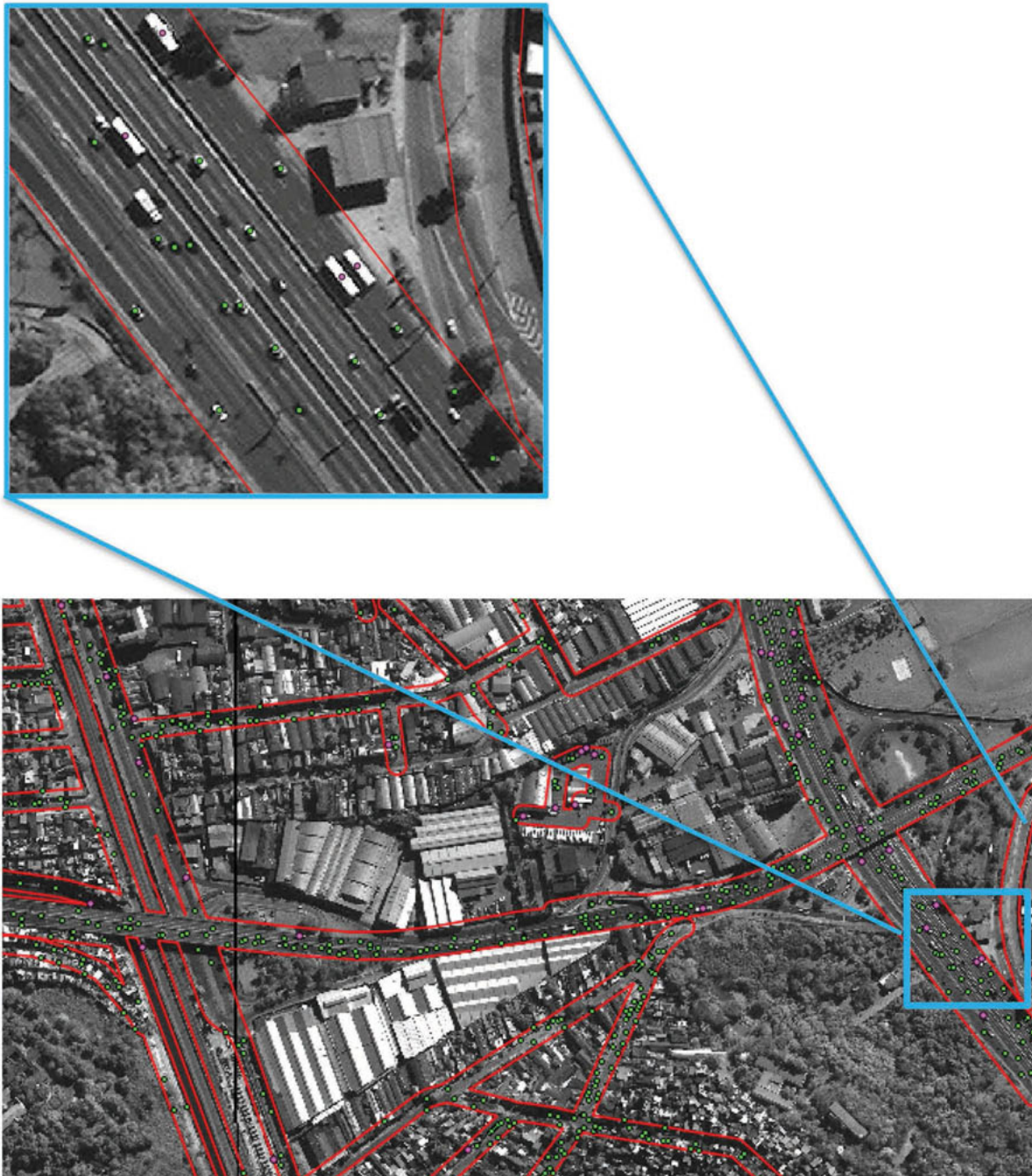
Available daily images for the Cairo region vary by size and centroid, so coverage differs greatly across grid cells. Some cells in central Cairo are covered by images for most days in the study period, while some cells at the metropolitan periphery have sparse coverage. To avoid problems due to cell coverage, we construct the largest possible balanced panel for estimation adopting the following procedure:

First, we rank grid cells by their image coverage counts. We begin with the top-ranked grid cell (C1). We construct a balanced panel with the second-ranking cell (C2), which entails some loss of observations from C1. If the gain exceeds the loss, we add the third-ranked cell (C3), construct the balanced panel for the three cells, and verify that the overall gain in observations exceeds the loss from adding C3. We continue this process until the loss exceeds the gain for the marginal grid cell. Construction of the largest possible balanced panel has resulted in 510 cells available for estimation, with 397 time-series observations per cell. The available satellite observations provide data for all twelve months, all days of the week, and hours from 10:00 AM to 2:00 PM daily (which is the period during which the satellites orbit over Greater Cairo). For a sample schematic of how cars were counted in downtown Cairo using the ML algorithm, refer to Figure 3. For more details, refer to the Technical Appendix.

²Orbital Insight.

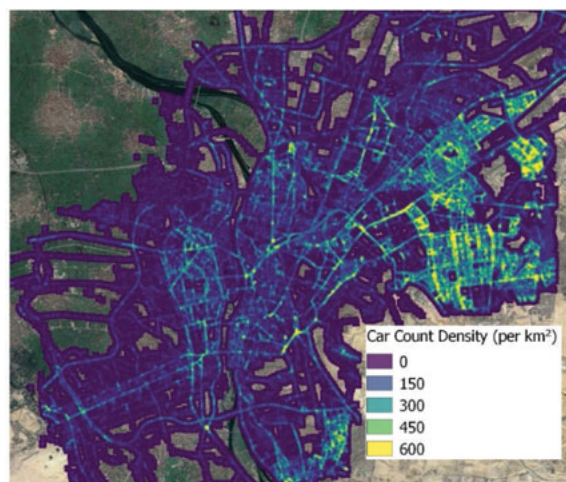
³Satellite imagery was available for Cairo for roughly 3–4 days per given week.

FIGURE 3: SCHEMATIC OF MACHINE LEARNING ALGORITHM DETECTING CARS IN THE STREETS OF CAIRO ON A STRETCH OF A HIGHWAY AND AT A NEIGHBORHOOD SCALE



The dataset employed in this article gives us the novel opportunity to directly infer the effects of various policies on traffic in Cairo without the need to rely on indirect measurements of driving behavior. The daily satellite images used in the dataset construction cover virtually the entire Greater Cairo area. Repeated observations over a period of ten years of the geo-referenced car detections make analysis with time series methods possible and enable the inference of medium-term effects on traffic characteristics and individual behavior.

FIGURE 4: CAR DENSITY IN THE STREETS OF CAIRO DURING AN AVERAGE WEEKDAY



Analyzing this comprehensive car data allows us to understand traffic patterns in the city and assess responses to policy shocks as well as linkages to air pollution. To our knowledge, this is the first satellite-derived car count dataset employed for environmental impact analysis.

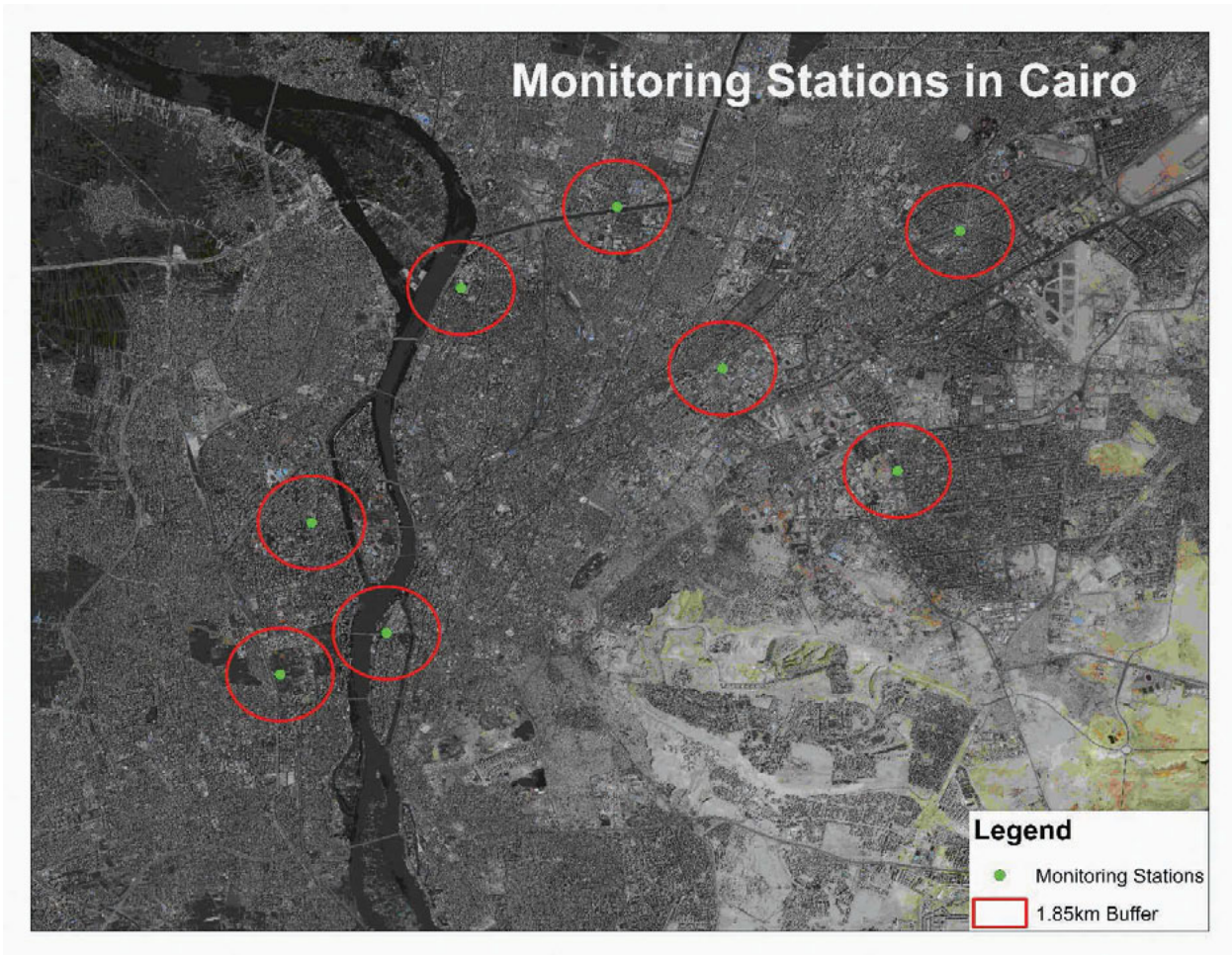
4.2 GROUND MONITORING AIR QUALITY MEASUREMENT

Air pollution data are collected using eight ground-monitoring stations in Cairo (see Figure 5). The stations log PM_{10} concentrations, along with other ambient air pollutants. The data itself has been provided by the Egyptian Environmental Affairs Agency and covers the years 2016 and 2017. This implies we cannot use the PM_{10} dataset for policy evaluation as the time series is not long enough.

4.3 INFORMATION ABOUT THE POLICY SHOCKS

We focus on four policy interventions: the phase-one opening of Cairo Metro Line 3 in February 2012; the phase-two opening of Line 3 in July 2014; a fuel price increase in November 2016, coupled with a simultaneous devaluation; and a fuel price increase in June 2017. The most recent years witnessed periods of significant economic volatility in Egypt, with relative stagnation in real income during the first years and more rapid growth subsequently. Significant interim events included a large devaluation in November 2016, and large, targeted fuel price increases in November 2016, and June 2017. These fuel price increases of 2016 and 2017 were quite large, varying between 30% and 80% by fuel category and period. *A priori* (based on the preceding), we would expect all of these events to have affected traffic volume significantly. Longer term fluctuations in real GDP should also have affected traffic via fuel purchases, new car purchases, maintenance intensity, and the retirement of older, fuel-inefficient cars. *A priori*, we expect these effects to produce positive, significant effects for real GDP.

FIGURE 5: LOCATION OF AIR QUALITY MONITORING STATIONS



Another policy intervention that may have been particularly significant for congestion and air pollution is Cairo’s Metro Line 3 opening during the sample period, with the phase-one opening of five stations in February 2012, and phase-two opening of an extension with four additional stations in May 2014 (Figure 6). By offering a rapid alternative to driving in this corridor, both openings may well have reduced traffic volume.

Given the nature of the event-based regression discontinuity approach, we only need information on the exact timing of the policy changes. This information is relatively easy to find employing online news portals such as Reuters or Al Jazeera. The exact dates we use are:

- | | |
|---------------------------|--------------------------------|
| » First fuel price shock | November 3, 2016 ⁴ |
| » Second fuel price shock | June 29, 2017 ⁵ |
| » Metro opening phase 1 | February 21, 2012 ⁶ |
| » Metro opening phase 2 | May 7, 2014 ⁷ |

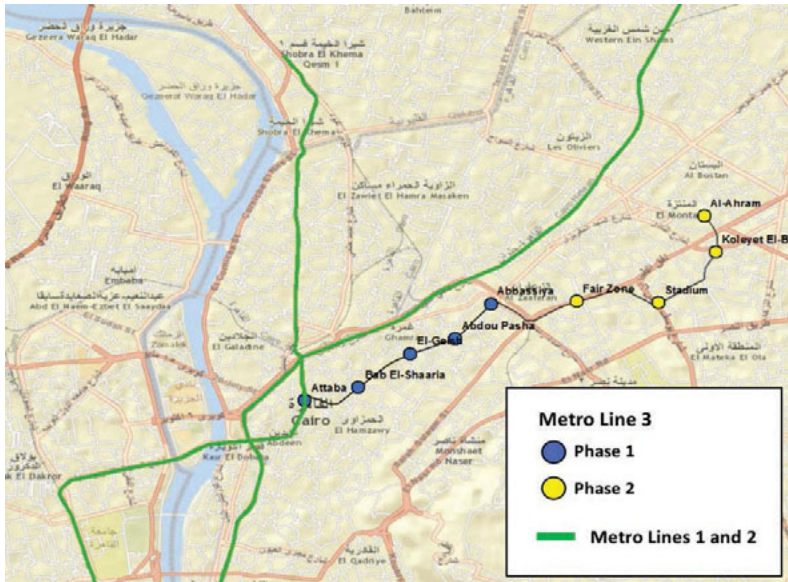
⁴<https://egyptianstreets.com/2016/11/04/gas-prices-increased-by-up-to-47-percent-in-egypt/>

⁵<https://www.reuters.com/article/egypt-economy-idUSL8N1JQ1G5>

⁶<https://www.vinci.com/vinci.nsf/en/press-releases/pages/20120222-0800.htm>

⁷<http://www.railwaygazette.com/news/news/africa/single-view/view/cairo-metro-line-3-extension-opens.html>

FIGURE 6: CAIRO METRO LINES



There was a third round of subsidy removal in 2018, which we were not able to evaluate as our dataset ends before then.

4.4 CONTROL VARIABLES

It is more than likely that traffic in Cairo is influenced by temporal regularities. For instance, we would expect more traffic during work days than on weekends. We also would expect different traffic patterns in summer and winter. In addition, car counts should vary considerably during the day. To control for these temporal patterns, we include a variety of time dummies in our regressions that control for hour, weekday, and month.

It is also possible that technical factors, such as different lenses or camera technologies of the sensors, lead to systematic differences in cars counted using imagery from different satellites. Thus, we include dummy variables for each of the four sensors used for this exercise.

To control for different cloud coverage on different days, we use the percentage of cloud coverage for each tile as a control. This variable has been computed directly from the raw satellite image.

We also include meteorological variables for our assessments of air pollution via the PM_{10} data collected by the Cairo measurement stations. For this exercise, we use data collected by a weather station located at the airport in Cairo. The station logs daily averages of temperature, relative humidity, and barometric pressure, as well as other meteorological variables (such as wind speed and wind direction), all of which may have a significant influence on pollution measures. We have collected the data via the Application Program Interface (API) of Weather Underground, a commercial weather service that compiles data both from official government sources and from private weather stations.

We control for aggregate income, which affects overall car counts via purchase, and scrap rates for the vehicle fleet. It also affects vehicle maintenance and operating rates, which are significant determinants of polluting emissions. The best available measure is the quarterly real GDP estimate provided by the Central Bank of Egypt. We perform quarterly smoothing, using a standard, seasonal dummy variable adjustment, and we interpolate between quarters to obtain monthly estimates. We adjust the model for a potentially important confounder—currency devaluation. At around the same time that the fuel subsidies were lifted, the Egyptian pound depreciated substantially, which may also have had an impact on the amount of demand for transportation. We posit that such a devaluation effect will register through changes in real GDP.

CHAPTER FIVE

RESULTS

This chapter presents the results of the policy impact on car density first (Section 5.1), followed by the relationship between car density and air pollution (Section 5.2). We find both evaluated policies significantly reduced car counts in Cairo. Furthermore, by extension of the estimated relationship between cars and PM_{10} levels in the Greater Cairo area, we conclude that the implemented policies also decreased air pollution levels in the city. A thorough impact analysis is carried out via counterfactual analysis.

5.1 THE IMPACT OF RECENT POLICY MEASURES ON TRAFFIC DENSITY IN CAIRO

Table 1 displays the complete results of the balanced panel estimation, with standard errors adjusted for clusters identified by grid cells. We include several variables to control for time patterns and trends. We include monthly dummies, with the exception of December, our reference month. The results show pronounced seasonal variation, with the highest car counts in June. Vehicle counts decline steadily from that seasonal high, reaching annual lows from November to January, and increasing again from February to May. The results of day-of-the-week dummies show that traffic volumes increase somewhat from Sunday to Tuesday, remain roughly constant through Thursday, decline sharply on Friday (as expected), and recover somewhat on Saturday. The dummy variable for 10:00 AM has been excluded from the hourly estimates. The results indicate that peak traffic volume (during the five hours of measurement) typically occurs around noon. The volume at 10:00 AM is significantly lower than the others. It increases to noon, and then decreases somewhat in the early afternoon.

We also include satellite technology factors. Among the five satellite platforms, we have excluded the dummy variable for “WorldView01.” *Ceteris paribus* (other things being equal), the three other platforms yield significantly higher counts, with the increment for “WorldView03” the largest by far. As expected, cloud cover percentage has a very large, highly significant effect on car counts.

After controlling for a host of temporal and technical factors, we are able to focus on the effects attributable to income and policy interventions. All estimated coefficients have the expected signs, and all are highly significant. Real GDP has a positive, highly-significant effect on traffic volume. Gaining 1 billion Egyptian pounds leads to an increase of about 1 car per tile. In 2017, quarterly GDP was 281 billion EGP. A 1% increase of GDP would

TABLE 1: FIXED-EFFECTS ESTIMATES (CLUSTER STANDARD ERRORS): DETERMINANTS OF CAIRO VEHICLE COUNTS PER CELL

Month	Coef/ t-stat	Day	Coef/ t-stat	Hour	Coef/ t-stat	Technical Factors	Coef/ t-stat	Event Factors	Coef/ t-stat
January	2.011 (2.19)*	Sunday	19.064 (8.07)**	11:00 AM	57.603 (27.54)**	GE01 Sat.	7.717 (7.63)**	Real GDP	0.952 (15.89)**
February	19.843 (14.93)**	Monday	22.562 (10.83)**	12:00 PM	92.368 (26.89)**	WV02 Sat.	12.209 (12.99)**	Metro Line 3 Phase 1	-24.67 (17.47)**
March	63.544 (21.12)**	Tuesday	25.944 (11.57)**	1:00 PM	61.031 (24.80)**	WV03 Sat.	92.399 (26.57)**	Metro Line 3 Phase 2	-15.35 (14.62)**
April	71.962 (20.21)**	Wednesday	23.134 (10.45)**	2:00 PM	69.515 (23.74)**			Fuel Price Hike Nov 3, 2016	-17.90 (14.32)**
May	97.186 (20.97)**	Thursday	26.647 (12.17)**					Fuel Price Hike June 29, 2017	-25.96 (21.83)**
June	117.46 (22.73)**	Friday	-43.75 (18.73)**			Cloud %	-141.0 (28.66)**		
July	87.957 (19.58)**							Constant	-108.6 (8.26)**
August	78.183 (21.37)**								
September	57.628 (20.42)**								
October	19.908 (14.28)**								
November	-16.41 (18.42)**								

Observations 202,470
Cells 510
Absolute value of t statistics in parentheses
* significant at 5%; ** significant at 1%

therefore result in 2.8 additional cars per tile. Since the Egyptian economy grew by about 20% between 2010 and 2017, GDP growth would have resulted in about 56 additional cars per tile. At the same time, the countervailing measures the government took decreased the number of cars in the streets.

On account of the metro openings, car counts decreased by 40 cars per tile. Reducing fuel subsidies resulted in 44 fewer cars per tile. This means that the policy actions succeeded in more than compensating for the congestion and air pollution due to GDP growth. For every 2 cars in the streets as a result of a growing economy, 3 cars have been taken off the streets by the policies.

A few additional notes are warranted with respect to possible threats to identification:

First, the fuel price increase of November 3, 2016, coincided with a major devaluation, so the estimated impact may incorporate some devaluation effects. To address this, we note again that a major part of the devaluation impact should be captured by real GDP in the model specification.

Second, we may well be underestimating the effects of the fuel price shocks. On the one hand, the Machine Learning algorithm counts parked as well as driving cars. Thus, even if people stop driving and park their cars at the side of the street, we do not capture that effect as the cars are still counted. Third, it is possible that the effects of the metro opening are biased upwards. We do not take into account that traffic congestion in the period before the metro opening might be elevated due to the metro construction. As a result, the metro policy coefficients might capture both the effects of removing the construction sites and the metro opening. However, as it is common procedure to have test runs of metro systems done for several months after the construction but before the public opening, we assume that this bias is of minor relevance.

Remaining threats to identification are other events that took place during the analyzed time period. However, to our knowledge, no major events that might affect traffic in Cairo have been neglected. For instance, Metro Line 3 opened one year after protests against Egypt's former president, Hosni Mubarak, were over, and one year before protests against his successor, Mohamed Morsi, flared up. Similarly, the Metro Line 3 extension opened more than a year after counterprotests against Morsi. To conclude, we are confident that our estimated impacts are thoroughly identified.

To summarize, our results provide very strong evidence that both fuel price increases and metro line openings have had significant impacts on traffic volume in Cairo. We should emphasize that these are persistent-effect estimates, which apply to the entire period from the policy events we study to the termination of our sample in September, 2017.⁸

5.1.1 TEMPORAL CONTEXT AND “FUNDAMENTAL LAW OF TRAFFIC CONGESTION”

The findings in Section 5.1 suggest that the policies implemented in Cairo do have significant effects on traffic in the long run. This contradicts what the so called “fundamental law of

⁸We have satellite-based car count observations through February 2018, but the real GDP series terminates in September 2017.

road congestion” (Duranton and Turner, 2011) would imply. The “fundamental law” states that new road capacity will be met with a proportional increase in driving. In other words, other cars will take the place of cars removed by the impact of mass transit. Introducing public transit is supposed to remove a significant number of cars from the streets. The fundamental law implies that, as the relative cost of driving increases, we should observe fewer cars on the roads as people switch to public transit. However, these effects should vanish in the longer run. This seems not to be the case in the Greater Cairo area for the time period that we analyze, according to the results in Section 5.1 that suggest significant long-term effects.

In line with the dynamics of the “fundamental law” we suppose there are significant, and strong, short-term effects that then decrease over time. This is that the analyzed metro openings should have large negative effects. When analyzing longer time windows, the effect size decreases as new cars take the place of the drivers that switched from private to public transport options. This would imply that the general idea of the “fundamental law” is valid, but the net effect of introducing public transit might not be zero in all metropolitan areas.

To test this hypothesis, we use the procedure introduced in Section 3. To gain insight regarding the short-term effects of the metro policies, we look at subsets of the residualized dataset that fall within various time windows around the metro opening dates. In particular, we start with a time window of ± 2 months,⁹ end at full dataset length, and analyze every time window in-between in steps of one month. This leaves us with over 90 separate models that allow us to compare the effect sizes when varying the time windows around the opening dates of metro phase 1 and phase 2.

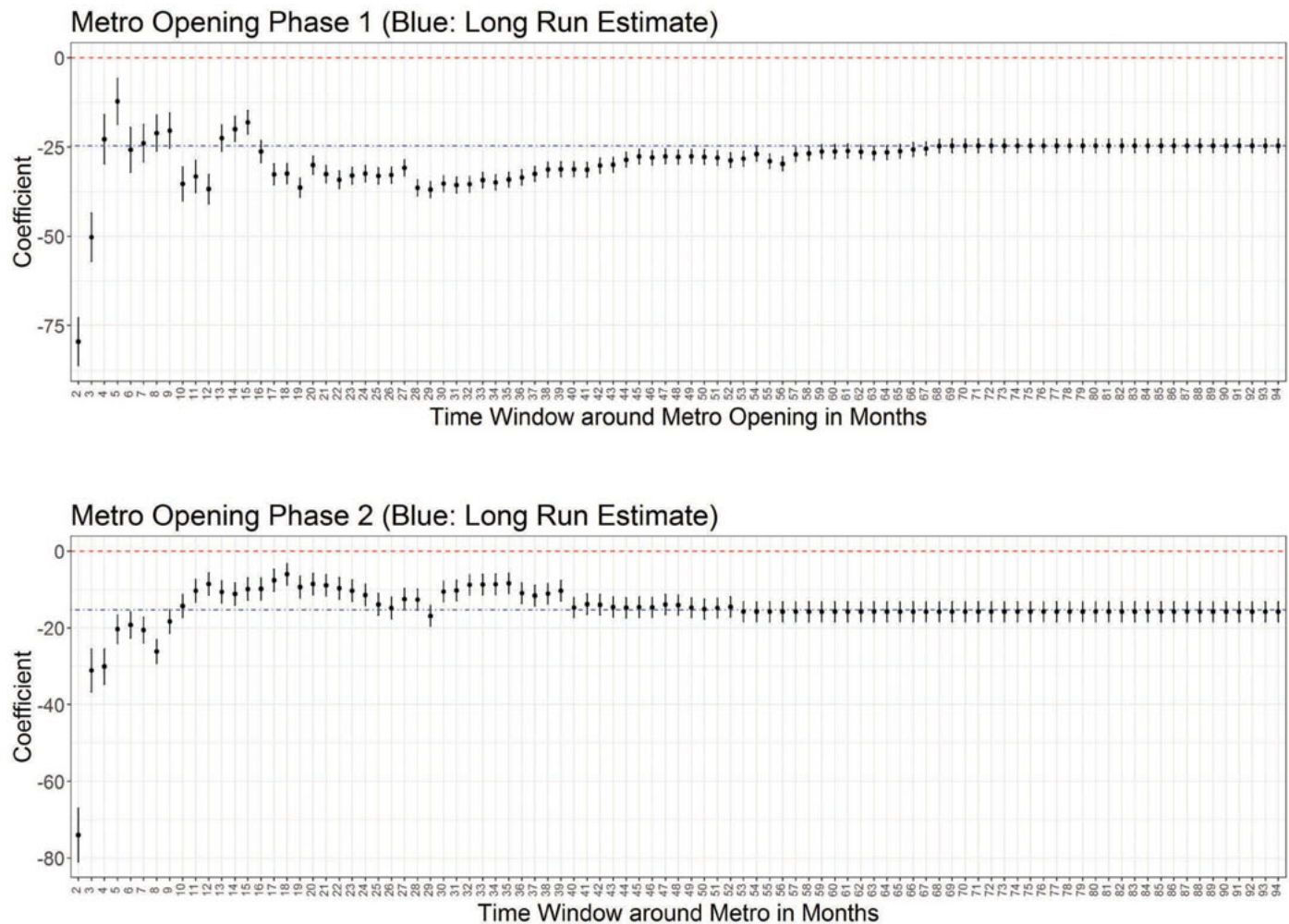
To summarize the results of the regression discontinuity models for all time windows, we provide the results of all estimations in Figure 7. The y-axis gives the estimated coefficient of the respective metro opening dummy, while the x-axis gives the analyzed time window in months. Every dot corresponds to the estimated coefficient of the metro opening dummy in one specific model. In addition, a 95% confidence interval of the effect size of the metro opening is provided for all estimated effects. The red line indicates the zero line. The blue line marks the estimated long run effect of the full model discussed in Section 5.1.

For both metro phases, the observed patterns suggest that the openings had strong negative effects in the very short term, which are then decreasing when using data from longer time periods. By construction, they converge to the long-term effects presented in Section 5.1. This seems to confirm our hypothesis that the time dynamics of the fundamental law hold.

Further research into possible reasons why Cairo shows a different behavior than the U.S. cities analyzed by Duranton and Turner (2011) will be necessary.

⁹Analyzing a shorter time window is not possible due to data restrictions.

FIGURE 7: ESTIMATED COEFFICIENTS AND 95% CIS FOR ALL TIME WINDOWS



In this section, we test the relationship between car densities and measured PM_{10} concentrations in Greater Cairo, while incorporating weather-related variables and dummy variables to incorporate technical, spatial, and temporal factors that we cannot observe directly.¹⁰ We have tried and discarded nonlinear specifications and quadratic and cubic spline specifications because they yield perverse results in this case.¹¹

¹⁰The modeled relationship is inherently linear, because it specifies atmospheric PM_{10} concentration in a fixed area as a function of cars operated within that area. The representative car emits a given quantity of particulates, and total vehicular particulate emissions are additive. Since particulate concentration is total particulate emissions divided by volume determined by a fixed area, the relationship between particulate concentration and car count is linear. Numerous real-world caveats apply, of course: Given a car count, total emissions also vary with car fleet composition within an area; combustion time per car, itself a function of car crowding in fixed road infrastructure; and weather factors not accounted for by monthly controls. Variations in local car fleet composition and weather are arguably random and seem unlikely to bias the estimated marginal relationship between car count and PM_{10} concentration. The potential role of combustion time is more complex. On one hand, variations in local road capacity will produce variations in congestion (and therefore combustion time) for identical car counts. On the other hand, the slope of the underlying relationship between car count and combustion time for a given road capacity must increase as cars progressively crowd into the streets. In the limit, traffic crawls toward gridlock and the marginal relationship between the slope and car count approaches infinity. If these relationships could be quantified by area, the appropriate righthand variable would be total combustion time. Vehicle count is our proxy, and our results therefore reflect “overall average traffic conditions” in the sample area.

¹¹These include extreme perverse changes in the estimated relationship near minimum and maximum values for car counts, as well as non-credible up-and-down fluctuations in the relationship for intermediate values. The linear spline function is stable and credible, but yields results that are nearly identical with pure linear estimation.

The dependent variable for each observation is the PM_{10} concentration reported by a monitor. The critical independent variable is the car density in the grid cells surrounding the monitor. Specifying the area radius involves balancing two factors. Vehicle density impacts on pollution presumably decline with distance from the monitor. On the other hand, mean density estimates are likely to be more stable and robust for larger areas.

The car count within each grid cell is specified at the cell centroid. With full area coverage by satellites, we would set an appropriate radius for the area bounding a PM_{10} monitor and simply count cars within that radius. This translates to vehicle density, given an invariant radius. However, satellite coverage of tiles varies by date in the database in the unbalanced panel. To compensate for variable coverage, we compute the mean for cells that are actually covered within the bounding area. Since cell sizes are identical, this also translates to vehicle density.

Variable coverage also has implications for the appropriate bounding radius. Ideally, the radius would be determined by prior scientific research on the relationship between distance-from-monitor and emissions impact on monitor readings. In practice, many location-specific variables may influence the calculation (for example, typical source emissions volume, wind speed, precipitation, and so on). In our case, variable satellite coverage introduces another complication. Suppose, for example, that the scientifically “optimal” radius is 0.5 km, but variable satellite coverage makes single-cell observations common within this radius. The result will be high variance in computed car-count means, which will in turn degrade the estimation of PM_{10} impacts. A larger radius would be better from a sampling perspective, since it would typically include more satellite-reported cells and more stable mean values. But, per the theoretical relationship, cells beyond the scientifically-optimal radius are more likely to introduce spurious elements into the calculation.

Here the optimization problem involves determining the intersection point of two curves: (1—upward sloping) the incremental sampling value of additional OI tiles covered by satellites; (2—downward sloping, with negative values beyond some point) the incremental value of measurements as their distance from the PM_{10} monitor increases.

For this exercise, we have imposed the assumption that the optimal point (the intersection of the two curves) is determined by the strongest statistical result. To test the balance, we have performed regression experiments for area radii from 1 to 5 km. We find that a radius of 1.85 kilometers yields the most robust result.

For model estimation, we introduce dummy variable controls for spatial and temporal factors. We assign a dummy variable to each monitoring station to control for technical measurement factors and other local unobserved emissions sources. We include five daily weather measures for the Cairo region: temperature, temperature lagged one day, barometric pressure, humidity, and wind speed. We also introduce a cloud cover correction for car counts. In a first-stage regression, we regress mean car density on mean cloud cover percent, along with dummy variables for the month, weekday, and hour of the observation. We also include dummy variables for PM_{10} stations, since mean vehicle density is likely to differ significantly across monitor areas. The regression fit is extremely strong, with high significance for all variable categories and a regression R^2 (adjusted for degrees of freedom) of 0.72. With the first-stage result in hand, we reset mean cloud cover to 0 for all observations and predict the adjusted “cloud-free” value of car density. We use cloud-adjusted car density for our regression exercise.

Table 2 reports our regression results. *Ceteris paribus*, PM_{10} readings differ substantially across monitors. The dummy variables for the Shubra Al Khaimah and M New monitoring stations have been excluded from the estimation to prevent total collinearity (more than one station dummy has been excluded because station dummies are also used in the cloud cover adjustment regression for car counts). As Table 2 shows, there are significant differences across stations after controlling for the other factors in the model.

July is excluded from the monthly dummy, so all monthly coefficients should be interpreted as deviations from the July result. The results indicate a relatively smooth pattern of seasonal variation, with the peak in December and the trough in May.

In contrast, the results by day-of-week and hour-of-day show little fluctuation, indicating that monitor readings do not fluctuate significantly during a typical week after accounting for the effect of car traffic. The same is true for hours during the day, with the exception of 11 AM. We should note again that dummy variables for some hours have been excluded to prevent total collinearity.

For this exercise, the most critical entry in Table 2 is the impact estimate for mean car counts in areas of 1.8 km radius around PM_{10} monitoring stations. We find a highly-significant effect: The measured PM_{10} concentration increases by $8.6 \mu\text{g}/\text{m}^3$ for every 100 cars added to a representative grid cell in the area surrounding the station monitor.¹² In our regression sample, cloud-adjusted car counts per cell vary from 19 to 714. Therefore, within the sample range, our coefficient estimate translates to potential induced changes in PM_{10} concentration of about $59 \mu\text{g}/\text{m}^3$.

¹²The estimated coefficient, .055, measures the increase in PM_{10} concentration per car. We have multiplied by 100 to obtain the estimate discussed above.

TABLE 2: CELL VEHICLE COUNTS AND PM₁₀ CONCENTRATIONS

PM ₁₀ Station	Coef/ t-stat	Month	Coef/ t-stat	Day	Coef/ t-stat	Hour	Weather	Coef/ t-stat	Vehicle Count ^a
Nasser Institute	-8.679 (1.14)	January	121.25 (3.92)**	Monday	-11.214 (1.20)	11:00 AM	Temp	0.729 (0.80)	0.086 (3.47)**
Al Ami Palace	-30.122 (4.18)**	February	97.45 (5.29)**	Tuesday	-14.407 (1.57)	2:00 PM	Temp_Lag	3.616 (4.02)**	
Abbasiyah	-49.79 (6.51)**	March	71.552 (3.88)**	Wednesday	-11.218 (1.29)		Pressure	-33.678 (1.15)	729.185 (0.80)
Nasr City	-51.952 (7.27)**	April	49.298 (3.24)**	Thursday	-14.901 (1.56)		Humidity	0.314 (0.97)	
Engineers	-28.158 (3.23)**	May	14.747 (1.05)	Friday	-4.002 (0.42)		Wind Speed	0.757 (0.83)	
Giza Square	-37.133 (4.68)**	June	21.331 (1.55)	Saturday	-17.885 (1.88)				
		August	11.123 (1.04)						
		September	39.272 (3.20)**						
		October	69.467 (4.30)**						
		November	67.313 (3.78)**						
		December	148.343 (6.27)**						

^aVehicle count adjusted for cloud cover
 Observations 499
 R-squared 0.33
 Absolute value of t statistics in parentheses
 * significant at 5%; ** significant at 1%

CHAPTER SIX

THE IMPACT OF (ENVIRONMENTAL)
POLICY ON CAR TRAFFIC, AIR POLLUTION,
AND HEALTH

We provide suggestive estimates on the overall policy impact using counterfactual simulation with controls for temporal and technical factors. Since our GDP series terminates in September 2017, we standardize on that month and year. We do the simulations for a typical Wednesday at 11 AM on a cloud-free day, for satellite platform WorldView02. We predict using real GDP in September 2017.

With all other model values fixed to the previously estimated values, we predict car counts for five cases: no intervening events (Metro 3 and the fuel price hikes never occurred; all dummy variables are 0), and each event included separately.

After obtaining predictions for 1,406 cells in the Cairo region, we sum the predictions. Table 2 reports our results, which suggest that the policies produced large reductions in the volume of traffic in central Cairo. With continued average income growth but no interventions, our results indicate that the midday car count for the region at 11 AM on a clear Wednesday in September 2017 would have been 434,673 cars. Our results indicate a car reduction of 56,275 attributable to the two metro openings and a reduction of 61,662 attributable to the two fuel price increases. With all four policy interventions, the car count under the same conditions is 316,735 cars—a reduction of 117,938 cars, or 27.1%.

The welfare implications of our results can be assessed in several dimensions. The first is economic: A 27.1% reduction in traffic volume implies a more-than-proportionate reduction in time-per-trip, since Cairo traffic must fit into the same road network in either case. As crowding rises and car speed falls, average time per trip and fuel cost per trip also rise. Thus, the large reduction in car load suggested by Table 1 generates large, aggregate, value-denominated welfare gains, via costs of fuel, maintenance, and depreciation, as well as the value of aggregate trip time saved.

Another critical factor in this context is environmental: Although more car-specific information would be valuable, it seems reasonable to assert that the greater-than-proportionate drop in congestion associated with a 12.9% decline in cars on account of the metro line, and 14.2% on account of the fuel price hike will also generate a reduction of vehicular pollutant emissions.

Table 3 provides a perspective on the relative significance of this estimate for PM₁₀ pollution in Cairo. The first column of the table reports the mean PM₁₀ concentration for each station

TABLE 3: CAIRO REGION: PROJECTED EVENT IMPACTS ON TRAFFIC VOLUME

Policy	Vehicle Reduction from Event	Percent Reduction
Public Transit		
Metro Phase 1 (2012)	34,692	8.0
Metro Phase 2	21,584	5.0
Public Transit Total	56,275	12.9
Price Incentives		
Fuel Price Increase + Devaluation (2016)	25,165	5.8
Fuel Price Increase (2017)	36,497	8.4
Price Incentive Total	61,662	14.2
Total Reduction	117,938	27.1
Total Vehicles without Events	434,673	
Total Vehicles with Events	316,735	

in the database for 2017. To produce the second column, we divide the mean PM_{10} concentration into the PM_{10} increment ($59 \mu g/m^3$) attributable to the maximum adjusted car count (714) in our sample. The resulting percentage is a measure of potential vehicular impact on air pollution in different areas of Cairo. The potential impact measure is very large in all cases, varying from 47.8% for the Nasser Institute station area to 73.9% for the Abbasiya station area (see Table 4).

Our results also provide a basis for estimating the impact of our four policy measures on PM_{10} pollution in Cairo. Table 5 displays our approach to estimation. Column 1 reproduces the Table 1 estimates of car count impacts per policy for a representative grid cell. In column 2, we multiply the car count impacts by .084, the Table 2 estimate of PM_{10} change per unit change in car count. Column 3 reports our counterfactual estimate of 2017 PM_{10} if none of the public transit or fuel price policies had been implemented. Column 4 sums columns 2 and 3 to estimate PM_{10} if each policy alone had been implemented. Column 5 converts

TABLE 4: CAIRO MONITORING STATIONS: POTENTIAL IMPACT MEASURE FOR PM_{10} ATTRIBUTABLE TO THE MAXIMUM SAMPLE CAR COUNT

Station Name	Mean PM_{10} , 2017 ($\mu g/m^3$)	Potential Impact Measure (%)
Abbasiya	79.8	73.9
Nasr City	82.8	71.3
Giza Square	87.7	67.3
Shubra Al Khaimah	8.8	66.4
Al Aini Palace	90.5	65.2
Nasser Institute	123.4	47.8

TABLE 5: ESTIMATED IMPACTS OF POLICY MEASURES ON CAIRO PM₁₀

Policy	Vehicle Count Impact (Table 1)	PM ₁₀ Change *.084 (Table 2)	PM ₁₀ w/o Transit or Price Policies (µg/m ³)	PM ₁₀ 2017 with Policy (µg/m ³)	Policy Impact on PM ₁₀ (%)
Public Transit					
Metro Phase 1 (2012)	-24.7	-2.1	98.5	96.4	2.1
Metro Phase 2 (2014)	-15.4	-1.3	98.5	97.2	1.3
Public Transit Total	-40.0	-3.4	98.5	95.1	3.4
Price Incentives					
Fuel Price Increase + Devaluation (2016)	-17.9	-1.5	98.5	97.0	1.6
Fuel Price Increase (2017)	-26.0	-2.2	98.5	96.3	2.3
Price Incentive Total	-43.9	-3.8	98.5	94.8	3.9
Overall Total	-83.9	-7.2	98.5	91.4	7.3

column 4 entries to estimated percentage reductions in PM₁₀. The table also includes summaries by policy category.

Our estimates imply an average 2017 PM₁₀ concentration of 98.5 µg/m³ if none of the policies had been implemented. Implementing the public transit policies alone would have reduced the concentration to 95.1 µg/m³ (a 3.4% decrease). If only fuel price incentives had been applied, PM₁₀ pollution would have fallen to 94.8 µg/m³ (a 3.9% decrease). Overall, our results suggest that the implementation of all four policies reduced annual average PM₁₀ by 7.2 µg/m³ (7.3%), to the actual 2017 mean of 91.5 µg/m³.

The Greater Cairo city-wide results reported in Tables 1 and 2 reflect a complex spatial pattern of adjustment. The basic economics of modal choice in urban transport provide some insights in this context. Over short periods, each household or business trip uses the mode that minimizes fully-accounted travel costs, given initial capital endowments, incomes, relevant prices, and residential and business locations. Travel cost components include fuel consumption, car depreciation, time in transit, comfort, and convenience. Holding all relevant variables constant, cost-minimizing travelers will explore iteratively until they reach an equilibrium distribution across existing transport modes. Travelers' short-term modal choices are interdependent, so a new equilibrium will not emerge instantaneously when an important background variable changes.

Over longer periods, exogeneity becomes endogeneity for capital endowments, incomes, residential and business locations, and at least some relevant prices. In the case of Cairo, which dominates the Egyptian economy, all relevant prices may actually be endogenous. The urban system will co-evolve with its constituent households and businesses, which may respond to an initial perturbation by changing locations, transactional venues, and car ownership propensities.

Given these complex temporal and spatial dynamics, no urban transport system ever attains static equilibrium. Background variables are always changing, and travelers are continually iterating interdependently across modal choices in response to cascading ripples of short- and long-run changes.

These complexities inevitably complicate any attempt to assess the benefits and costs of a policy intervention that affects one or more background variables. The first major problem is the demarcation of the bounding space for the analysis. Focusing on one area within a city may yield misleading or even perverse results, even if the intervention is welfare improving for the system as a whole. To cite one example, consider the potential whole-system response to extension of an existing subway system. This represents a major perturbation, with potential system-wide consequences for modal choice, traffic congestion, local incomes and prices, and the pattern of residential and business location. One major objective of the subway extension may be reduced motor car congestion, and this may well happen for the urban system as a whole. However, nothing guarantees this result for the area contiguous to the new subway line. In fact, the system's new equilibrium "solution" might even entail an increase in congestion in the entire system. In other words, the reduction of traffic in Cairo might come at the cost of increased traffic in the outskirts. It could very well be that the new metro stations incentivized more people living outside of Cairo to drive to a metro station, which would have led to an increase in traffic in the outskirts. In any case, the underlying message seems clear: Assessing the benefits and costs of a whole-system perturbation requires a system-scale analysis.

The second major problem also relates to the choice of bounding space, but this time at the urban margin. The outer boundary of a city is arbitrary, because the transaction space is continuous. Thus, one likely result of a major perturbation, such as a subway extension, will be the expansion of the area within which transactions density is sufficient to warrant its inclusion in the "city." For this reason, use of a city's current delineation as the bounding space for analysis may also result in miscalculation of overall benefits and costs.

A third complication relates to the temporal framework of the analysis. In the short and medium term, convergence toward a new post-intervention equilibrium may largely reflect the existing patterns of location, asset ownership, incomes and prices. Thus, a medium-term analysis (on the order of, say, six months to one year) might yield a pronounced impact on car congestion within a city. Over the longer term, given the induced changes in household and business location, asset ownership, income, and prices, the system may "absorb" some of the initially-observed congestion impact, effectively transforming it into more diffuse impacts across many variables that are relevant for a general accounting of welfare change.

Nothing in the previous paragraphs should be taken to imply that any transport-related intervention will ultimately be "self-neutralizing." In fact, our multiyear econometric results for Cairo (Tables 1 and 2) suggest the contrary.

Taken together, these propositions suggest that any intervention welfare analysis will be strongly influenced by its spatial and temporal bounds. The spatial bounds in this case are determined by the limitations of the car counts available from satellite imagery.

6.1 ILLUSTRATIVE EVENTS IN CAIRO

As illustrations, we consider two of the events featured in our analysis: the phase-one opening of Metro Line 3 and the fuel price increase of November 2016. In each case, we first generate the spatial distribution of cell-specific car counts for the longest period in which other study events do not intervene. For the fuel price increase of November 2016, the constraining factor is another price increase in June 2017. Accordingly, our prior and posterior observations are bounded by November 3 to the following June 28, for periods starting in 2015 and 2016, respectively. For the Metro 3 phase one opening, our intervals are the prior and posterior years (February 21, 2011, to February 20, 2012, and February 21, 2012, to February 20, 2013), respectively). For each prior period, we compute mean car counts by cell. For each posterior period, we make an adjustment from our regression results to incorporate the effect of changing real income. Starting from actual posterior means by cell, we reduce all observations in constant proportions so that the mean difference between prior and posterior counts is equal to the relevant regression coefficient in Table 1. To reiterate, this adjustment is necessary because the “raw” posterior measures incorporate the confounding effects of interim income growth (and, possibly, other unobserved factors).

The result provides a rough approximation to the change in the spatial distribution of car counts that is attributable to a policy measure, after correcting for the interim effects of income growth.

Phase 1 of Cairo’s Metro Line 3 opened on February 21, 2012. Table 6 displays the overall distribution of car counts before and after this event (the strength and significance of the suggested attribution is tested in the econometric model), after the adjustments described above. The distribution of changes exhibits a clear skew toward declines, which occur in about 75% of the 1,406 grid cells tabulated. The mean decline is 24.8 cars which, as previously noted, we have designed to produce a near-match with the regression coefficient for Metro 3 phase 1 in Table 1.

TABLE 6: METRO LINE 3 PHASE 1 OPENING, FEB 21, 2012

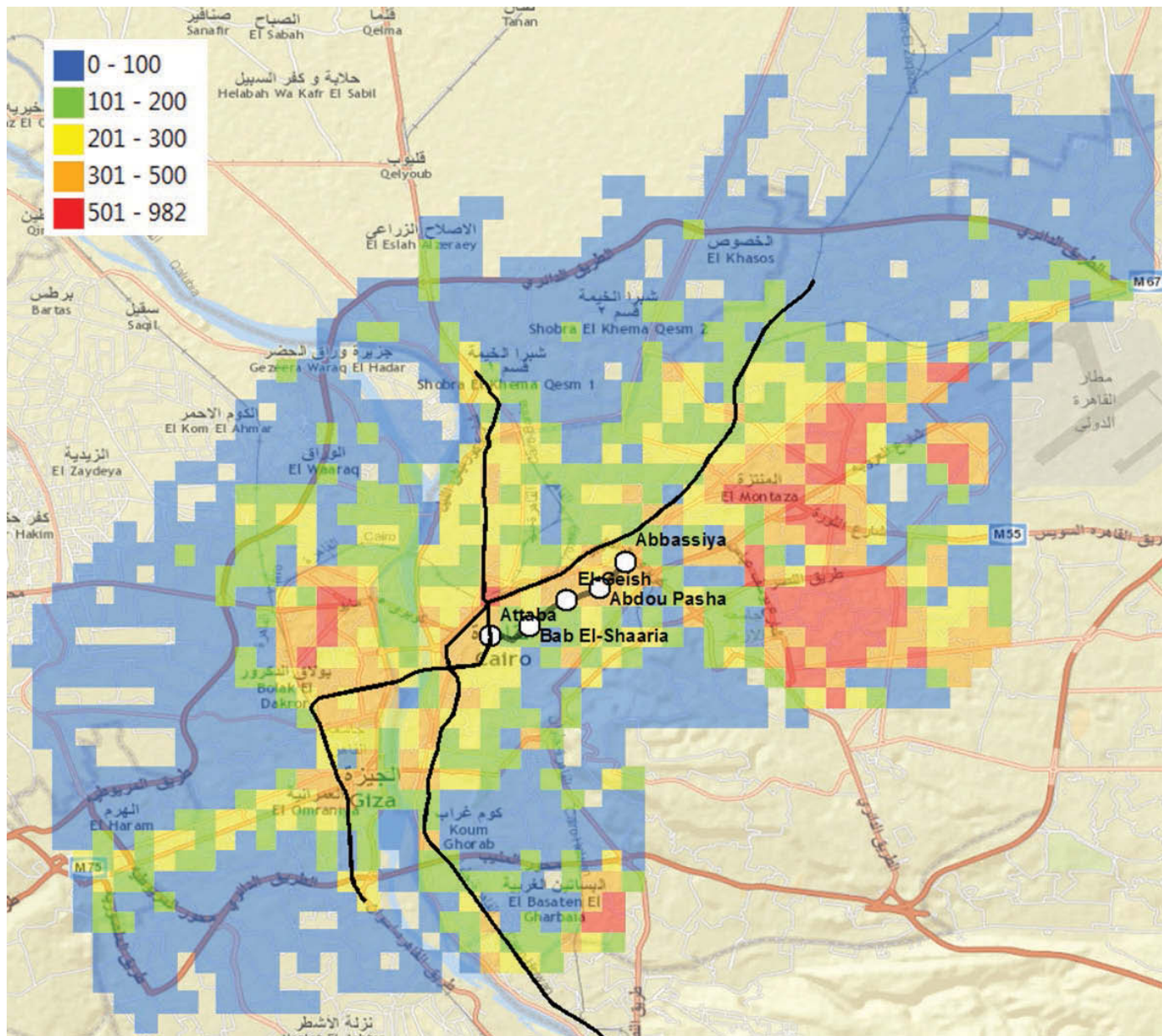
Ex-ante (Feb. 21, 2011–Feb. 20, 2012)

Ex-post (Feb. 21, 2012–Feb. 20, 2013)

[Vehicle counts per grid cell]

	Ex-Ante Means	Ex-Post Means	Distribution of Changes
N	1,406	1,406	1,406
min	0.0	0.0	–250.1
p10	4.8	4.4	–66.5
p25	22.8	19.5	–35.8
p50	80.2	67.4	–12.6
mean	140.1	115.4	–24.8
p75	204.2	167.0	–1.6
p90	364.7	296.0	0.8
max	873.3	683.7	104.6

FIGURE 8A: SPATIAL DISTRIBUTION OF CAR COUNTS PRIOR TO THE METRO 3 PHASE ONE OPENING



Figures 8a and 8b display the spatial distributions for ex-ante cell means and the simulated changes induced by the metro opening. In each figure, changes are color-coded by cell and overlaid on a Cairo map that includes the five stations included in the phase one opening.

Figure 8a clearly shows Cairo’s “core congestion” in an upward-canted area extending from west to east. Two large areas of particularly intense congestion are colored red. Outside of those areas, car counts display a declining gradient from the core congestion axis.

FIGURE 8B: SPATIAL DISTRIBUTION OF CAR COUNT CHANGES AFTER THE PHASE ONE OPENING

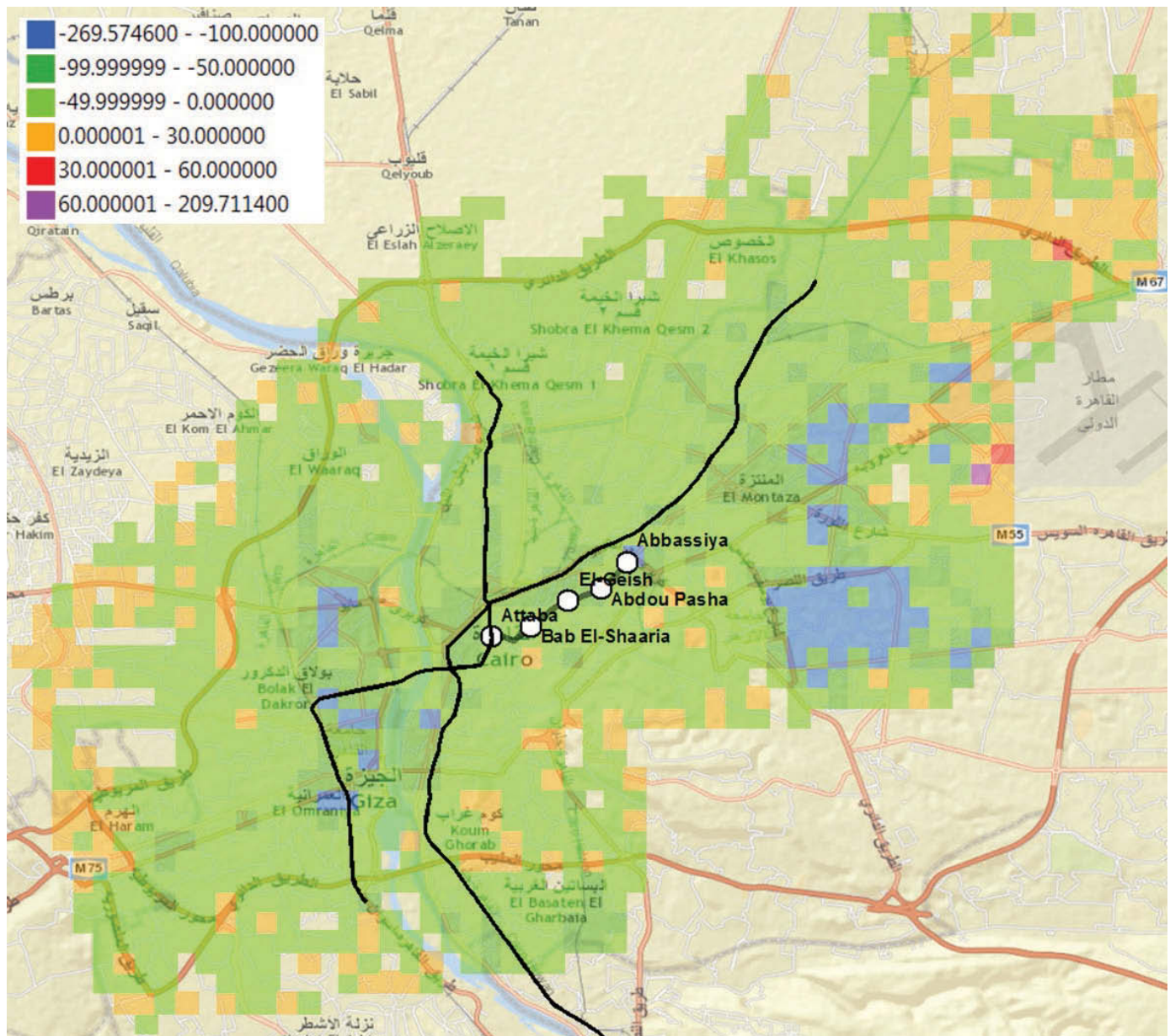


Figure 8b displays the simulated pattern of changes after the phase one opening of Metro Line 3. Here the system-wide consequences of the opening are clearly apparent. While car counts decline in the area surrounding the new metro extension, they also decline throughout the region—and particularly in the areas of highest prior congestion (colored red in Figure 8a).

TABLE 7: FUEL PRICE INCREASE, NOVEMBER 3, 2016: EX-ANTE AND EX-POST CAR DENSITIES

[Vehicle counts per grid cell]			
	Ex-Ante Means	Ex-Post Means	Distribution of Changes
N	1,404	1,404	1,404
min	0.0	0.0	−269.6
p10	5.7	7.0	−82.8
p25	26.1	29.6	−30.6
p50	90.8	87.3	−4.0
mean	160.8	142.8	−18.0
p75	237.2	205.5	3.1
p90	420.1	356.8	19.2
max	982.2	809.4	209.7

FUEL PRICE INCREASE, 2016

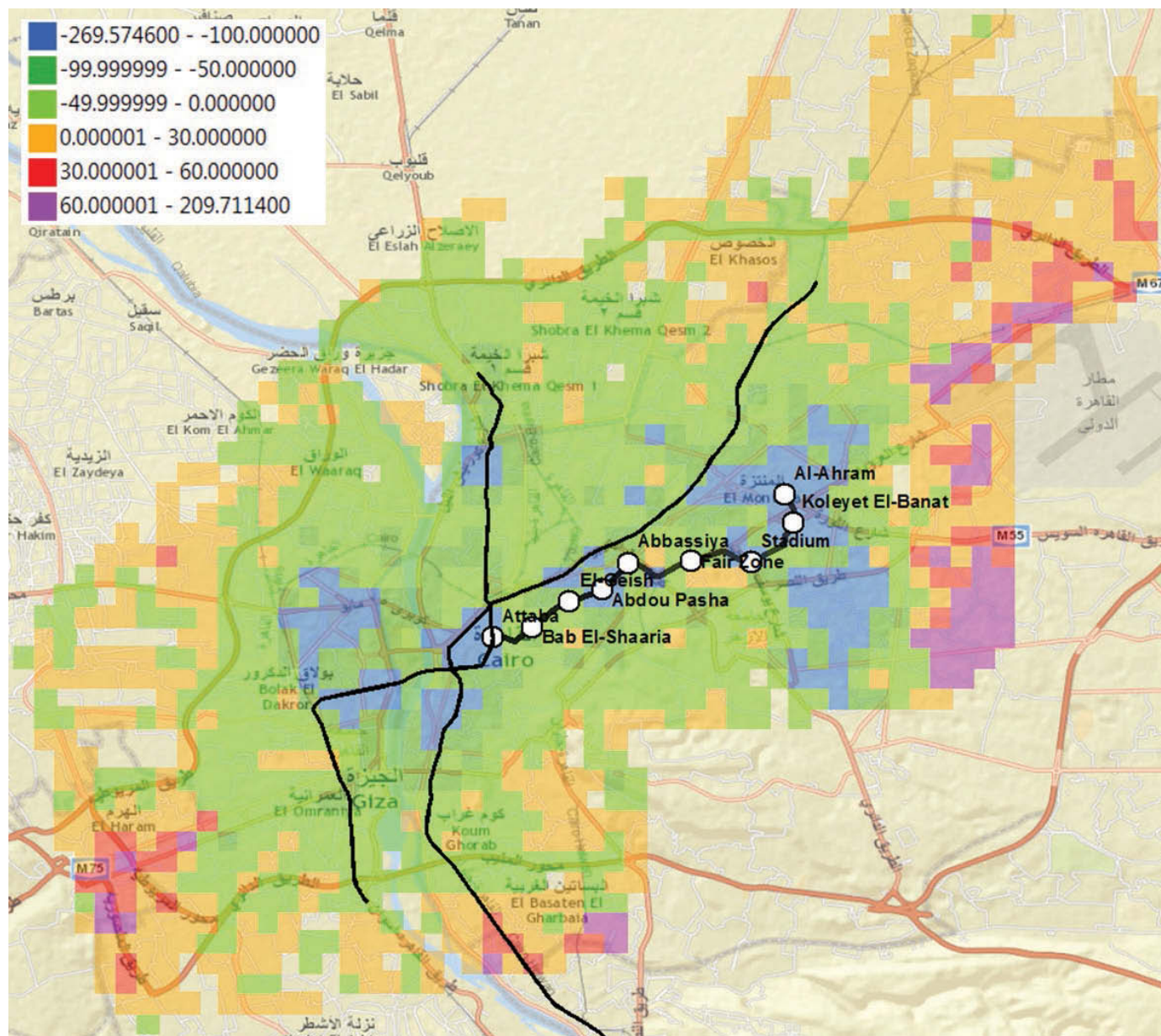
On November 3, 2016, the Egyptian government implemented fuel price increases that varied from 30% to 50% across categories. In Table 7, substantially more than half of the 1,404 grid cells tabulated exhibit declines in the aftermath of the fuel price shock.¹³ Again, we have adjusted the posterior results to achieve parity with the associated regression result in Table 1.

Figures 9a and 9b display the spatial patterns of ex-ante cell means and ex-post changes. Figure 9a closely resembles Figure 8a, showing the same axial “core congestion” region surrounded by areas with declining congestion gradients. However, Figure 9b is considerably different than Figure 8b. In Figure 9b, blue-colored areas with the greatest declines in car counts are much more pervasive and spread all along the core congestion axis. In counterpoint, Figure 9b also shows pervasive increases in car counts along the eastern and western peripheries of the region. These results have two implications that could be explored through more in-depth analysis. First, as indicated by the difference in regression coefficients in Table 1, the overall decline in traffic attributable to the phase one opening of Metro Line 3 is larger and generally more widespread than the decline attributable to the fuel price increase. However, the spatial pattern of adjustment to the fuel price increase appears to be more complex, with greater spatial clustering of both increases and decreases in vehicle density.

¹³As previously noted, for the purposes of this discussion we assign the impact of the simultaneous devaluation to our measure of real income.

[illegible]

FIGURE 9B: SPATIAL DISTRIBUTION OF CAR COUNT CHANGES AFTER THE NOVEMBER 3 INCREASE



6.2 VALUE OF HEALTH BENEFITS RESULTING FROM PM₁₀ REDUCTION

The monetary valuation of the effects of the policies due to the reduction in particulate matter is a question of high policy relevance. For this exercise, we employ a procedure that is similar to the analysis presented in Gendron-Carrier et al. (2018). The underlying rationale is to quantify the benefits that result from lower air pollution, employing the relationship of air pollution and infant deaths and the concept, value of statistical life (VSL).

As Gendron-Carrier et al. (2018) point out, it can be seen as a rule of thumb that a 1 µg/m³ decrease in PM₁₀ concentration will avert around 10 infant deaths per 100,000 births. This value is derived from various articles that estimate this relationship. For instance, Arceo et al. (2016) estimate this number to be 12.5 for Mexico City, while Knittel et al. (2016) estimate 9.9 for California. Chay and Greenstone (2003) find that in the U.S., 9.5 infant deaths can be averted by reducing PM₁₀ particle counts by 1 µg/m³. We assume that this number will approximately hold in our geo-temporal setting as well.¹⁴

The results of this exercise will depend on the functional form of the relationship of infant mortality and air pollution. However, estimates of the dose response relationship between PM₁₀ particles and infant mortality for high pollution environments like Cairo are rare. Samoli et al. (2005) estimate a linear relationship until PM₁₀ concentrations reach around 150 µg/m³. This also corresponds to the average PM₁₀ concentration in Greater Cairo (Safar and Labib, 2010). For values larger than 150 µg/m³, Samoli et al. (2005) find a more than proportional effect of PM₁₀ concentration on mortality for Southern European countries. We assume that similar results will hold for child mortality in Egypt and assume a linear relationship to produce conservative results.

Using this rationale together with our estimates, it is straightforward to infer the monetary value of the health benefits that are due to the policies discussed in this article. The number of infant deaths averted can be calculated as

$$\text{Reduction in PM}_{10} * (10 * 10^{(-5)}) * \text{Birthrate} * \text{Population}$$

The reduction in PM₁₀ particles has been derived as 7.2 µg/m³. We assume that the birth-rates of Egypt and Cairo are the same. The World Bank Development Indicator database suggests an average birthrate of 27.30 children per 1,000 individuals for the time frame from 2009 to 2016 (the most recent observation available). The average population of Cairo between 2010 and 2018 was 18.50 m according to the UN World Urbanization Prospects. Using these values, we conclude that the policies implemented by the government of Egypt averted the death of 364 infants.

Viscusi and Masterman (2017) present new estimates of the value of statistical life that are used in this analysis. Assuming that the effects due to the policies are of permanent nature, the country-adjusted VSL for Egypt (\$575,000) suggests a monetary value of \$209.1 m attached to the averted infant deaths. The independent contribution of only the metro openings (−3.4 µg/m³) can be evaluated at a value of \$98.7 m using the same methodology. Relating

¹⁴For a review of the topic, refer to Gendron-Carrier et al. (2018), Section 7.

this number to the cost of the Metro Line 3 infrastructure opened so far,¹⁵ the infant mortality effects alone account for 7.69% of the construction costs.

Please note that this benefit analysis neither includes reductions in labor productivity nor morbidity due to, for instance, respiratory diseases. We also do not look into other particle pollutants like NO_x or PM_{2.5}. Hence, it is obvious that the estimated value of the health benefits of the implemented policies has to be seen as low comparative to the range of possible values.

¹⁵Phase 1 cost approximately \$700 m, phase 2 approximately \$585 m according to various newspaper articles.

CHAPTER SEVEN

SUMMARY AND CONCLUSIONS

This report used high-resolution data on car counts from satellite imagery to investigate the relationships linking Cairo traffic, PM₁₀ air pollution, and a series of policy measures that have affected Cairo traffic and environmental quality in recent years. We have focused on four policy interventions: the phase-one opening of Cairo Metro Line 3 in February 2012; the phase-two opening of Line 3 in July 2014; a fuel price increase in November 2016, coupled with a simultaneous devaluation; and a fuel price increase in June 2017.

Our first econometric exercise uses fixed-effects panel estimation to assess the effects on Cairo traffic of changes in real income, and the four policy interventions. We measure Cairo traffic using time series of car counts for 1,406 grid cells with sides of 0.006 degrees (approximately 660 meters).

We find high significance and substantial coefficient size estimates for all of the temporal, technical, economic, and policy variables in the model. Vehicle counts vary systematically by month, day-of-week, and hour; across satellite observation platforms; and with cloud cover. Real GDP has the expected positive, sizable effect on car counts. Finally, we find significant negative impacts for all four policy interventions.

A second econometric exercise indicates significant, persistent measurement differences across PM₁₀ monitoring stations and significant variations by month. We find little variation by day-of-week and hour-of-day after controlling for the other variables. Our result for car counts is both highly significant and meaningfully large: an increase of 8.6 $\mu\text{g}/\text{m}^3$ for each increase of 100 in cars counted in a grid cell. Since the car counts in our sample vary from 0 to 714, the implied potential variation from car counts alone is 59 $\mu\text{g}/\text{m}^3$. We compare this magnitude with mean 2017 PM₁₀ measures for six stations with available data and find that within-sample variations in car counts are sufficient to produce very large percentage changes in typical station measures.

Finally, we combine our econometric results for car counts and PM₁₀ concentrations to estimate the impacts of our four policy interventions on air quality in Cairo. The estimated impacts are proportional to the estimated reductions in car counts estimated for the policy interventions by our panel estimation exercise. When the intervention impacts are combined, they produce a Cairo PM₁₀ concentration that is about 7.3% lower than the counterfactual concentration. The order of magnitude of this result is in line with the results of other national and global studies cited in our discussion of previous research. We demonstrate that national macroeconomic policy, targeted price incentives, and public transit investments have all been very important determinants of Cairo's air quality.

REFERENCES

- Abou-Ali, H., and Thomas, A. 2011. Regulating Traffic to Reduce Air Pollution in Greater Cairo, Egypt. In Economic Research Forum Working Papers (No. 664).
- Adler, M. W., and van Ommeren, J. N. 2016. Does public transit reduce car travel externalities? Quasi-natural experiments' evidence from transit strikes. *Journal of Urban Economics*, 92, 106–119.
- Anderson, M. L. 2014. Subways, strikes, and slowdowns: The impacts of public transit on traffic congestion. *American Economic Review*, 104(9), 2763–96.
- Arceo, E., Hanna, R., and Oliva, P. 2016. Does the effect of pollution on infant mortality differ between developing and developed countries? Evidence from Mexico City. *The Economic Journal*, 126(591), 257–280.
- Basagaña, X., Triguero-Mas, M., Agis, D., Pérez, N., Reche, C., Alastuey, A., and Querol, X. 2018. Effect of public transport strikes on air pollution levels in Barcelona (Spain). *Science of The Total Environment*, 610, 1076–1082.
- Chay, K. Y., and Greenstone, M. 2003. Air quality, infant mortality, and the Clean Air Act of 1970 (No. w10053). National Bureau of Economic Research.
- Chen, Y., and Whalley, A. 2012. Green infrastructure: The effects of urban rail transit on air quality. *American Economic Journal: Economic Policy*, 4(1), 58–97.
- Congressional Budget Office (CBO). 2008. Effects of Gasoline Prices on Driving Behavior and Vehicle Markets. Congress of the United States.
- Crowther, Geoffrey, Holford, William, Kerensky, Oleg, Pollard, Herbert, Smith, T. Dan, and Wells, Henry W. 1963. Traffic in Towns. London: HMSO.
- Dargay, J. M., and Vythoulkas, P. C. 1999. Estimation of a dynamic car ownership model: a pseudo-panel approach. *Journal of Transport Economics and Policy*, 287–301.
- Duranton, G., and Turner, M. A. 2011. The fundamental law of road congestion: Evidence from US cities. *American Economic Review*, 101(6), 2616–52.
- Fridstrøm, L. 1998. An econometric model of aggregate car ownership and road use. In 8th World Conference on Transport Research (WCTR), Antwerp, Belgium.
- Gendron-Carrier, N., Gonzalez-Navarro, M., Polloni, S., and Turner, M. A. 2018. Subways and urban air pollution (No. w24183). National Bureau of Economic Research.
- Gillingham, K. 2014. Identifying the elasticity of driving: evidence from a gasoline price shock in California. *Regional Science and Urban Economics*, 47, 13–24.

- Goel, D., and Gupta, S. 2014. The effect of metro rail on air pollution in Delhi (No. 229). Working paper.
- Goodwin, P., Dargay, J., and Hanly, M. 2004. Elasticities of road traffic and fuel consumption with respect to price and income: a review. *Transport reviews*, 24(3), 275–292.
- Graham, D. J., and Glaister, S. 2002. The demand for automobile fuel: a survey of elasticities. *Journal of Transport Economics and Policy*, 1–25.
- Knittel, C. R., Miller, D. L., and Sanders, N. J. 2016. Caution, drivers! Children present: Traffic, pollution, and infant health. *Review of Economics and Statistics*, 98(2), 350–366.
- Lalive, R., Luechinger, S., and Schmutzler, A. 2017. Does expanding regional train service reduce air pollution? *Journal of Environmental Economics and Management*.
- Lovell, M. C. 2008. A simple proof of the FWL theorem. *The Journal of Economic Education*, 39(1), 88–91.
- Pang, J. 2018. Do Subways Reduce Congestion? Evidence from US Cities. Working Paper. <https://drive.google.com/file/d/0B7gPhmW3MkVAZXR5VDVLdWZDMIE/view>. Accessed June 13, 2018.
- Pendyala, R. 2010. Reflecting the impact of fluctuating fuel prices on travel behavior in the context of regional model improvements and dynamic simulations. Maricopa Association of Governments. Available at: http://azmag.gov/Portals/0/Documents/TRANS_2010-12-16_Final-Report-Reflecting-The-Impact-of-Fluctuating-Fuel-Prices-On-Travel-Behavior.pdf?ver=2017-04-06-111939-653. Accessed June 13, 2018.
- Rivers, N., and Plumptre, B. 2016. The effectiveness of public transit subsidies on ridership and the environment: Evidence from Canada.
- Rivers, N., Saberian, S., and Schaufele, B. 2017. Public Transit and Air Pollution. Available at SSRN: <https://ssrn.com/abstract=3049945> or <http://dx.doi.org/10.2139/ssrn.3049945>
- Safar, Z. S., and Labib, M. W. 2010. Assessment of particulate matter and lead levels in the Greater Cairo area for the period 1998–2007. *Journal of Advanced Research*, 1(1), 53–63.
- Samoli, E., Analitis, A., Touloumi, G., Schwartz, J., Anderson, H. R., Sunyer, J., . . . , and Goodman, P. 2005. Estimating the exposure–response relationships between particulate matter and mortality within the APHEA multicity project. *Environmental Health Perspectives*, 113(1), 88.
- Tabatabaiee, S. A., and Rahman, A. 2011. The effect of Urban rail transit on decreasing energy consumption and air pollution in Ahvaz City. In *Advanced materials research* (Vol. 255, pp. 2802–2805). Trans Tech Publications.
- Thomas, A. 2016. Reducing air pollution in Cairo: Raise user costs and invest in public transit. Economic Research Forum Policy Briefs, 12, 1–6.
- Viscusi, W. K., and Masterman, C. J. 2017. Income Elasticities and Global Values of a Statistical Life. *Journal of Benefit-Cost Analysis*, 8(2), 226–250.
- Wang, Haidong, Laura Dwyer-Lindgren, Katherine T. Lofgren, Julie Knoll Rajaratnam, Jacob R. Marcus, Alison Levin-Rector, Carly E. Levitz, Alan D. Lopez, and Christopher J. L. Murray. 2012. “Age-specific and sex-specific mortality in 187 countries, 1970–2010: a systematic analysis for the Global Burden of Disease Study 2010.” In: *The Lancet* 380.9859, pp. 2071–2094.
- World Bank. 2010. Egypt—Cairo traffic congestion study—phase 1 (English). Washington, DC: World Bank.

- World Bank. 2013. Egypt—For better or for worse: air pollution in Greater Cairo: sector note (English). Washington, DC: World Bank.
- Yang, J., Chen, S., Qin, P., Lu, F., and Liu, A. A. 2018. The effect of subway expansions on vehicle congestion: Evidence from Beijing. *Journal of Environmental Economics and Management*, 88, 114–133.
- Zheng, S., Zhang, X., Sun, W., and Wang, J. 2017. The effect of a new subway line on local air quality: A case study in Changsha. *Transportation Research Part D: Transport and Environment*.

TECHNICAL APPENDIX

A1. VEHICLE COUNTS

The authors partnered with a remote sensing company (Orbital Insight), which applied a trained Machine Learning (ML) algorithm to satellite imagery of Cairo, counting every car in the metropolis’s streets for each day (satellite imagery was available for Cairo for roughly 3 to 4 days per given week) from January 2010 to April 2018. For a sample schematic of how cars were counted in downtown Cairo using the ML algorithm, refer to Figure A1.

The data product has been provided by Orbital Insight in a gridded format; the grid over Cairo is depicted in Figure A1.

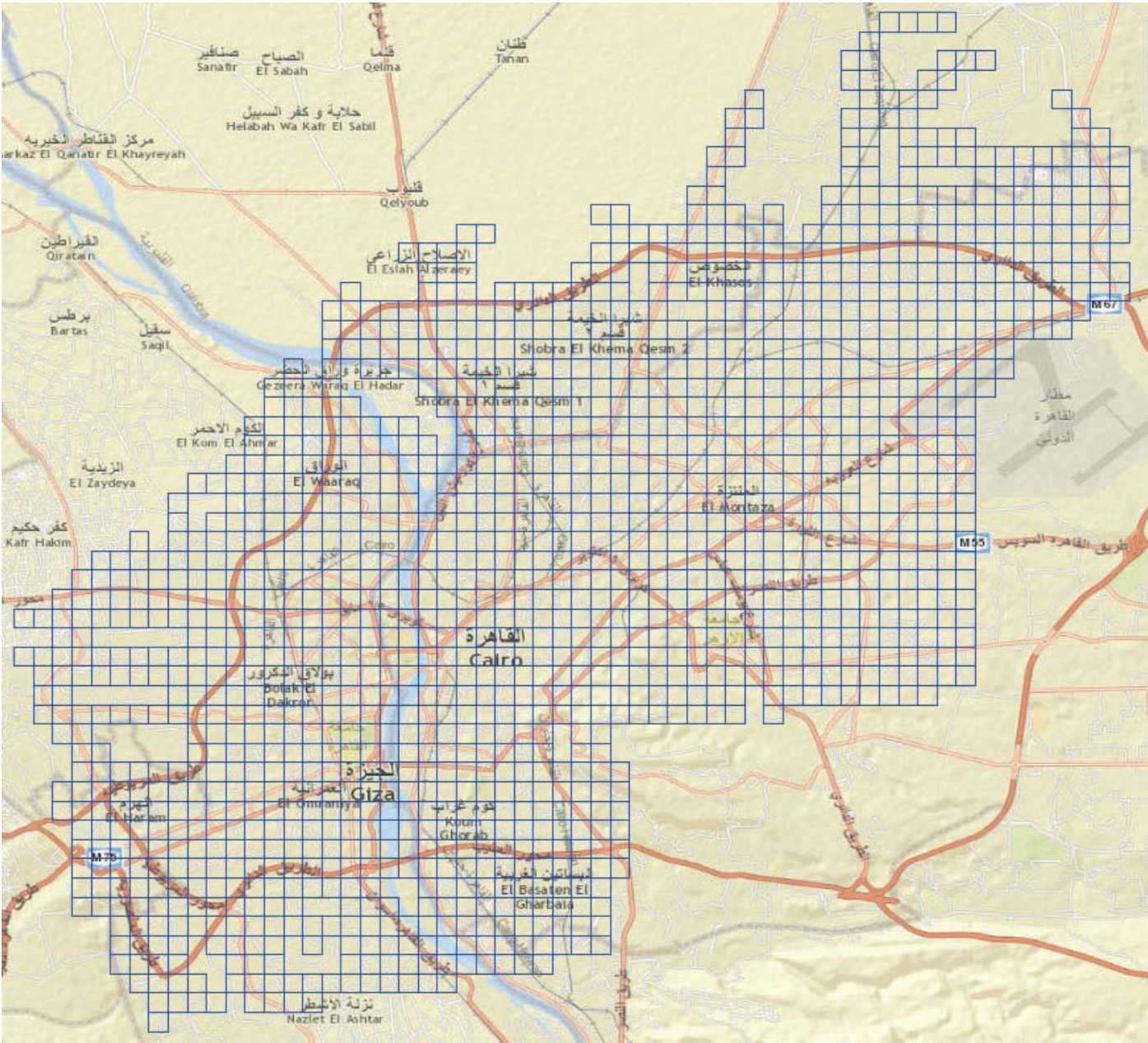
A2. SATELLITES

Cars were counted based on satellite imagery obtained from five different satellites. Table A1 indicates the number of images processed per satellite. Each count is from a different year.

TABLE A1: IMAGE COUNTS PER SATELLITE

Sensor	Image Count
WorldView02	235
WorldView01	202
WorldView03	120
GeoEye 1	57
Quickbird 2	50

FIGURE A1: GRID OVERLAY IN GREATER CAIRO



1. ACCURACY ASSESSMENT OF CAR COUNTS

Because we contracted a remote sensing company to create the results from scratch, we developed an accuracy assessment for the trained Machine Learning algorithm. We compare the cars identified by the ML algorithm and cars we identify from visual inspection. In the accuracy assessment we focus on the ratio of false negatives (that is, cars that are recognized as such by the human eye according to visual inspection but are not counted by the ML algorithm) relative to cars that are both recognized as such by the human eye and the artificial intelligence eye.

The car counting results have high quality for all the WorldView sensors, as a comparison between manual car counts and Machine Learning algorithm car counts shows in Table A2, despite the occasional false positives (as for example with WorldView01 satellite) or the occasional false negative (as for example displayed by WorldView02 and WorldView03 satellites). However, the Quickbird imagery appears to have a much lower degree of accuracy. These varying degrees of accuracy across satellites indicate the importance of controlling for satellites in our regression specifications. Given the apparent inaccuracy of the Quickbird 2 in this context, we have decided to drop that imagery for this exercise.

TABLE A2: ACCURACY ASSESSMENT

Sensor	Manual Car Count	Machine Learning Car Count
WorldView02	430	400
WorldView01	115	138
WorldView03	821	801
GeoEye 1	NA	NA
Quickbird 2	1,316	560



1818 H Street, NW
Washington, D.C. 20433 USA
Telephone: 202-473-1000
Internet: www.worldbank.org/environment